Innovative Instrumentation and Analysis of the Temperature Measurement for High Temperature Gasification

Final Technical Report

Reporting Period Starting Date: 10/01/02
Reporting Period End Date: 09/30/06

Principal Author(s): Dr. Seong W. Lee

Date Report was issued: October 2006

DOE Award Number: DE-PS26-02NT41681

Name and Address of Submitting Organization:
Morgan State University
School of Engineering
5200 Perring Parkway
Baltimore, MD 21239

DISCLAIMER

This report was prepared as an account of work sponsored by an agency of the United States Government. Neither the United States Government nor any agency thereof, nor any of their employees, makes any warranty, express or implies, or assumes any legal liability or responsibility for the accuracy, completeness, or usefulness of any information, apparatus, product, or process disclosed, or represents that its use would not infringe privately owned rights. Reference herein to any specific commercial product, process, or service by trade name, trademark, manufacturer, or otherwise does not necessarily constitute or imply its endorsement, recommendation, or favoring by the United States Government or any agency thereof. The views and opinions of authors expressed herein do not necessarily state or reflect those of the United States Government or any agency thereof.

ABSTRACT

The project entitled, "Innovative Instrumentation and Analysis of the Temperature Measurement for High Temperature Gasification", was successfully completed by the Principal Investigator, Dr. S. Lee and his research team in the Center for Advanced Energy Systems and Environmental Control Technologies at Morgan State University. The major results and outcomes were presented in semi-annual progress reports and annual project review meetings/presentations.

Specifically, the literature survey including the gasifier temperature measurement, the ultrasonic application in cleaning application, and spray coating process and the gasifier simulator (cold model) testing has been successfully conducted during the first year. The results show that four factors (blower voltage, ultrasonic application, injection time intervals, particle weight) were considered as significant factors that affect the temperature measurement. Then the gasifier simulator (hot model) design and the fabrication as well as the systematic tests on hot model were completed to test the significant factors on temperature measurement in the second year. The advanced Industrial analytic methods such as statistics-based experimental design, analysis of variance (ANOVA) and regression methods were applied in the hot model tests. The results show that operational parameters (i.e. air flow rate, water flow rate, fine dust particle amount, ammonia addition) presented significant impact on the temperature measurement inside the gasifier simulator. The experimental design and ANOVA are very efficient way to design and analyze the experiments. The results show that the air flow rate and fine dust particle amount are statistically significant to the temperature measurement. The regression model provided the functional relation between the temperature and these factors with substantial accuracy. In the last year of the project period, the ultrasonic and subsonic cleaning methods and coating

materials were tested/applied on the thermocouple cleaning according to the proposed approach. Different frequency, application time and power of the ultrasonic/subsonic output were tested. The results show that the ultrasonic approach is one of the best methods to clean the thermocouple tips during the routine operation of the gasifier. In addition, the real time data acquisition system was also designed and applied in the experiments. This advanced instrumentation provided the efficient and accurate data acquisition for this project.

In summary, the accomplishment of the project provided useful information of the ultrasonic cleaning method applied in thermocouple tip cleaning. The temperature measurement could be much improved both in accuracy and duration provided that the proposed approach is widely used in the gasification facilities.

Table of Contents

List of Figures

List of Tables

Appendix II

1. Introduction

It is well known that gasification offers the cleanest, most efficient method available to produce synthesis gas from low or negative-value carbon-based feed stocks such as coal, petroleum coke, high sulfur fuel oil or materials that would otherwise be disposed as waste. The gas can be used in place of natural gas to generate electricity or as a basic raw material to produce chemicals and liquid fuels. Tomorrow's power fleet likely will be increasingly comprised of advanced plants that gasify coal rather than burning it. Operating the coal gasifier at exactly the right temperature - optimized for both the plant equipment and the type of coal will be a key factor in efficient operation. In addition, optimum efficiency translates directly into low costs of electric power to consumers or low cost liquid fuels and chemicals that can be made from the coal gas. Coal gasification can be used to produce three primary products: low, medium and high BTU gases [1].

The high temperature in gasifiers converts the inorganic materials in the feedstock (such as ash and metals) into a vitrified material resembling coarse sand. Within some feedstocks, valuable metals are concentrated and recovered for reuse. The vitrified material, generally referred to as slag, is inert and has a variety of uses in the construction and building industries.

Gas treatment facilities refine the raw gas using proven commercial technologies that are an integral part of the gasification plant. Trace elements or other impurities are removed from the syngas and are either re-circulated to the gasifier or recovered. Sulfur is recovered either in its elemental form or as sulfuric acid, both marketable commodities.

If the syngas is to be used to produce electricity, it is typically used as a fuel in an integrated gasification combined cycle (IGCC) power generation configuration. IGCC is the cleanest, most efficient means of producing electricity from coal, petroleum residues and other

low- or negative-value feed stocks.

All the operating gasifiers are equipped with temperature instrumentation. Normally, the regular temperature measurement techniques such as heat expansion thermometers and regular thermocouples are used in these gasifiers. However, temperature measurement in gasification is always a problem because the current methods are not robust and reliable in the harsh gasifiers environment. Based on the DOE Gasification Database Results Update 2001 [2,3], there are more than 800 gasifiers operating in the United States. Most of them suffer from unreliable temperature measurement, which can trigger false alarms, lower the gas quality and create accidents. Since most of the existing and planned gasifiers are used to or will be used to generate electricity in IGCC, cost rules similar to those used for power plants can be applied to the operation of these gasifiers.

Any feasible instrumentation for temperature measurement in gasifiers will be operated for a long time (at least 150 hours) in an environment, which contains granular carbonaceous material, sticky and/or molten ash and gas containing significant quantities of methane, water vapor, carbon monoxide and hydrogen. Also, low concentrations of alkali metals, hydrogen sulfide, hydrogen chloride and ammonia can be found in the environment.

In order to develop the proposed instrumentation successfully, it is essential to design a corresponding cold and hot gasification models to test the proposed instrumentation.

Because of the harsh environment in gasifiers and the high cost of developing temperature measurement device on a full scale gasifier, a feasible approach normally starts with a small scale cold model. The cold model testing shall provide tremendous information at a much lower cost.

After the cold model tests are successfully completed, a hot model shall be made to test the temperature measurement device. These hot model tests shall provide the accurate results of the temperature measurement device that could be used directly into the full-scale testing. The cold model and hot model tests are the most cost efficient way to study or develop applications in a full scale unit.

The objective of this research is to develop innovative instrumentation and analysis for high temperature measurement in gasification using the specialized thermocouple along with two cleaning methods. Basically, ultrasonic dirt peeling and high-pressure oxygen injection cleaning are the two methods proposed to clean the thermocouple tip for accurate and robust measurement. The anti-erosion/corrosion coating sprayed on the thermocouple could make the thermocouple specialized and unique. The proposed instrumentation is believed to be low-cost and reliable. Finally, this research work is expected to reduce a significant amount of the operation/maintenance costs and increase the gas production rate [2, 3].

2. EXECUTIVE SUMMARY

The literature on the temperature measurement and cleaning methods of the gasifier system were extensively surveyed. The cold model and hot model of the gasifier systems were designed, fabricated and integrated for systematic tests. The statistic techniques of design of experiment, analysis of variance and regression analyses were applied in this project. The gasifier hot model was designed and fabricated in accordance to the proposed schedule. The gasifier simulator body is made of carbon steel pipe of 24-inch high and 8-inch outer diameter. The thickness of the gasifier is 0.25-inch. The electric hearing coil is installed inside the gasifier chamber. The heating element of the heating coil is L17-10 nichrome wire coil which can heat the insider materials up to 1200^{o}C with 3 kW of inputted electric power. The refractory layer and cooling water lines are attached to the I side and outsider of the wall to maintain the inside temperature and outside temperature as requirement.

The cold model tests on four (4) factors including blower voltage, ultrasonic application, injection time intervals, and the particle weight were considered as the significant factors that affect the temperature measurement. The analysis of variance was applied to analyze the test data. The analysis shows that all four factors are significant to the temperature measurements in the gasifier simulator. The regression analysis for the case with the normalized room temperature shows that for the linear model the temperature data fits with 82% accuracy. The regression analysis indicates a better fit than that of the linear regression. The nonlinear regression model's accuracy is 88.7% for normalized room temperature. Based on the cold model testing and its analysis, it was found that normalized room temperature was a great help to analyzed the experimental data in gasifier simulator tests.

The vibration application for cleaning purpose was explored. Both ultrasonic and sub-sonic vibration were considered for this research application. The ultrasonic vibration frequency is above 20khz. The sub-sonic vibration frequency is below 20khz. The 2^2 factorial design was selected to design the experiments to study the impact of the vibration on temperature measurement. The vibration was created by using a high-speed motor with an unbalanced mass at the motor shaft. The two factors, temperature and motor speed, were set to two levels respectively. Motor speeds were set as two levels, 3000 rpm and 6000 rpm. These two motor speeds corresponded to 50 HZ and 100 HZ respectively. Three (3) temperature readings were recorded when the temperature approached stable temperature. From the ANOVA, it was found that the vibration had no significant impact on the temperature measurement for any temperature levels in the gasifier simulator. The interaction between the vibration and temperature levels was also not significant. So it is believed that thermocouple vibration had no significant impact on the temperature measurements in the gasifier simulator.

The systematic tests of the ultrasonic vibration application on cleaning effect were conducted both in ambient temperature and high temperature. Four (4) factors were considered as the potential parameters affecting the peeling rate of vibration. The four factors include the different shapes of the cement-covered layers (i.e. thickness and length), the ultrasonic vibration output power, and application time. At the high temperature tests, four (4) different environments were considered as the experimental parameters: (i) air flow supply, (ii) water and air supply environment, (iii) water, air, and fine dust particle supply, and (iv) air, water, ammonia, and fine dust particle supply environment. The factorial design method was used for the experimental design along with twelve (12) data sets of readings. Analysis of Variances (ANOVA) results showed that the thickness and length of the cement-covered layer had the significant impact on

the peeling off rate of ultrasonic vibration application at the ambient temperature environment. For the high temperature tests, the different environments do not seem to have significant impact on the temperature changes. These results may indicate that the ultrasonic vibration is one of the best cleaning methods for thermocouple tip cleaning in high temperature gasification.

The effect of high velocity oxygen fuel (HVOF) spray coating on the temperature measurement was tested. The coated thermal couple and uncoated thermal couple were amounted together to measure the temperature at the same location. The temperature changes along with the experimental time were recorded. The computerized data acquisition system (DAS) was adopted to record the temperature data accurately. The operational conditions are the combination of three parameters: (1) air flow rate, (2) water/ammonia flow rate and (3) the amount of fine dust particles. Each parameter has two (2) levels. A total of eight experiments were scheduled according to the full factorial design matrix. The results from the temperature readings show the temperature of uncoated thermal couple is uniformly higher than that of coated thermal couple for each operational condition. It is believed that the coating layer will increase the heat resistance between the thermal couple tip and the object. The increased heat resistance differs the temperature measurement. The ANOVA results show that there are no significant factors or interactions affecting the temperature readings at the type I error of α=0.05, which indicates that the coated thermal couple could be applied to the temperature measurements in the gasifier. Therefore, it is concluded that the coated thermal couple could be used to measure the temperature in the reducing and harsh environment.

3. Literature Review

3.1 Gasification and Gasifier

The gasification process converts any carbon-containing material into a synthesis gas composed primarily of carbon monoxide and hydrogen, which can be used as a fuel to generate electricity or steam or used as a basic chemical building block for a large number of uses in the petrochemical and refining industries [4]. Gasification adds value to low- or negative-value feed stocks by converting them to marketable fuels and products.

Gasification technologies differ in many aspects but share certain general production characteristics. Typical raw materials used in gasification are coal, petroleum based materials (crude oil, high sulphur fuel oil, petroleum coke, and other refinery residuals), gases, or materials that would otherwise be disposed of as waste. The feedstock is prepared and fed to the gasifier. The feedstock reacts in the gasifier with steam and oxygen at high temperature and pressure in a reducing (oxygen starved) atmosphere. This produces the synthesis gas, or syngas, made up primarily of carbon monoxide and hydrogen (more than 85% by volume) and smaller quantities of carbon dioxide and methane. The high temperature in the gasifier converts the inorganic materials in the feedstock (such as ash and metals) into a vitrified material resembling coarse sand. With some feedstocks, valuable metals are concentrated and recovered for reuse. The vitrified material, generally referred to slag, is inert and has a variety of uses in the construction industries. There are various kinds of gasifiers available in the market. Among them, air blown fixed-bed and fluidized-bed gasifiers appear to have several advantages for biomass power systems [5]. The oxidant for the gasification process can be either atmospheric air or pure oxygen. Oxygen-blown gasifiers offer a higher-Btu gas and faster reaction rates than air-blown systems, but have the disadvantage of additional capital costs associated with the oxygen plant.

3.2 Erosion and Corrosion in Gasifier

Many potential biomass feedstocks, such as straw and many fast-growing energy crops as well as industrial and municipal waste fuels often contain high amounts of chlorine, and alkali metals or aluminum, which have a tendency to cause severe corrosion and fouling problems in boiler [6,7].

Corrosion may be a problem, especially on surfaces in the high temperature areas of the gasifier (the throat). These corrosions can be caused by too high temperatures and/or contaminants in the feedstock. The gasifier design should be adapted to lower the temperature and/or to use other heat resistant materials. Before the produced gas can be used in a gas engine or turbine, it has to be cooled and cleaned from tars, alkaline metals and dust. Tars may condensate on valves and fittings hampering the valves to function properly; alkaline metals, dust and tars cause corrosion and erosion of cylinder walls and pistons. When the gas is used in heat applications the requirements on gas quality are not much strict, especially when the gas remains at high temperatures during transportation to the burner, which prevents tars and alkaline metals to condensate.

3.3 Current Temperature Measurement in Gasifiers

Thermocouples are often used in the gasifiers to measure the temperature. The big challenge is how to keep the thermal couple tip clean [8,9]. Reliable measurement of temperature in gasifier is important for the proper operation of slagging, entrained-flow gasification processes. Thermocouples have been widely used as the main measurement technique, and the temperature inferred from syngas methane concentration being used as a backup measurement. While these have been sufficient for plant operation in many cases, both techniques suffer from limitations. The response time of methane measurements is too slow to detect rapid upset

conditions and thermocouples are subject to long-term drift, as well as slag attack, which eventually leads to failure of measurement. Texaco's Montebello Technology Center (MTC) has developed an infrared ratio pyrometer system for measuring gasifier reaction chamber temperature. This system has a faster response time than both methane and thermocouples, and has been demonstrated to provide reliable temperature measurements for longer periods of time when compared to thermocouples installed in the same MTC gasifier. In addition, the system can be applied to commercial gasifiers without any significant scale-up problems. The major equipment items, the purge system and the safety shutdown system in a commercial plant will be essentially identical to the prototypes at MTC.

3.4 Ultrasonic Cleaning

Ultrasonic cleaning involves the use of high-frequency sound waves (above the upper range of human hearing, or about 18 kHz) to remove a variety of contaminants from parts immersed in aqueous media [10]. The contaminants can be dirt, oil, grease, buffing/polishing compounds, and mold release agents, just to name a few. Materials that can be cleaned include metals, glass, ceramics, and so on. In a process termed cavitations, micron-size bubbles form and grow due to alternating positive and negative pressure waves in a solution. The bubbles subjected to these alternating pressure waves continue to grow until they reach resonant size. Just prior to the bubble implosion, there is a tremendous amount of energy stored inside the bubble itself.

Temperature inside a cavitations bubble can be extremely high, with pressures up to 500 atm. The implosion event, when it occurs near a hard surface, changes the bubble into a jet about one-tenth the bubble size, which travels at speeds up to 400 km/hr toward the hard surface. With the combination of pressure, temperature, and velocity, the jet frees contaminants from their

bonds with the substrate. Because of the inherently small size of the jet and the relatively high energy, ultrasonic cleaning has the ability to reach into small crevices and remove entrapped soils very effectively. An excellent demonstration of this phenomenon is to take two flat glass microscope slides, put lipstick on a side of one, place the other slide over top, and wrap the slides with a rubber band. When the slides are placed into an ultrasonic bath with nothing more than a mild detergent and hot water, within a few minutes the process of cavitation will work the lipstick out from between the slide assembly. It is the powerful scrubbing action and the extremely small size of the jet action that enable this to happen. In order to produce the positive and negative pressure waves in the aqueous medium, a mechanical vibrating device is required. Ultrasonic manufacturers make use of a diaphragm attached to high-frequency transducers. The transducers, which vibrate at their resonant frequency due to a high-frequency electronic generator source, induce amplified vibration of the diaphragm. This amplified vibration is the source of positive and negative pressure waves that propagate through the solution in the tank. The operation is similar to the operation of a loudspeaker except that it occurs at higher frequencies. When transmitted through water, these pressure waves create the cavitation processes.

The resonant frequency of the transducer determines the size and magnitude of the resonant bubbles. Typically, ultrasonic transducers used in the cleaning industry range in frequency from 20 kHz to 80 kHz. The lower frequencies create larger bubbles with more energy, as can be seen by dipping a piece of heavy-duty aluminum foil in a tank. The lower-frequency cleaners will tend to form larger dents, whereas higher frequency cleaners form much smaller dents.

The basic components of an ultrasonic cleaning system include a bank of ultrasonic transducers mounted to a radiating diaphragm, an electrical generator, and a tank filled with aqueous solution. A key component is the transducer that generates the high-frequency mechanical energy. There are two types of ultrasonic transducers used in the industry, piezoelectric and magnetostrictive. Both have the same functional objective, but the two types have dramatically different performance characteristics. The ultrasonic generator converts a standard electrical frequency of 60 Hz into the high frequencies required in ultrasonic transmission, generally in the range of 20 kHz to 80 kHz. Many of the better generators today use advanced technologies such as sweep frequency and autofollow circuitry. Frequency sweep circuitry drives the transducers between a bandwidth slightly greater and slightly less than the center frequency. For example, a transducer designed to run at 30 kHz will be driven by a generator that sweeps between 29 kHz and 31 kHz. This technology eliminates the standing waves and hot spots in the tank that are characteristic of older, fixed-frequency generators. Autofollow circuitry is designed to maintain the center frequency when the ultrasonic tank is subjected to varying load conditions. When parts are placed in the tank or when the water level changes, the load on the generator changes. With autofollow circuitry, the generator matches electrically with the mechanical load, providing optimum output at all times to the ultrasonic tank.

The safety issues for the ultrasonic application are also under investigation. Human exposure to ultrasonic with frequencies between 16 kHz and 100 kHz can be divided into three distinct categories: airborne conduction, direct contact through a liquid coupling medium, and direct contact with a vibrating solid. Ultrasonic through airborne conduction does not appear to pose a significant health hazard to humans. However, exposure to the associated high volumes

of audible sound can produce a variety of effects, including fatigue, headaches, nausea and tinnitus. When ultrasonic equipment is operated in the laboratory, the apparatus must be enclosed in a 2-cm thick wooden box or in a box lined with acoustically absorbing foam or tiles to substantially reduce acoustic emissions (most of which are inaudible). Direct contact of the body with liquids or solids subjected to high-intensity ultrasonic of the sort used to promote chemical reactions should be avoided. Under sonochemical conditions, cavitation is created in liquids, and it can induce high-energy chemistry in liquids and tissues. Cell death from membrane disruption can occur even at relatively low acoustic intensities. Exposure to ultrasonically vibrating solids, such as an acoustic horn, can lead to rapid frictional heating and potentially severe burns.

3.5 High Velocity Oxygen Flame Coating Process

The High Velocity Oxygen Flame (HVOF) coatings are used in applications requiring the highest density and strength not found in most other thermal spray processes [11]. HVOF Spraying is essentially a variation of powder flame spraying in which a modified torch is used to constrict the gas flow. This produces an extremely high velocity flame that is similar to that of a jet engine. HVOF coatings are usually denser and have higher bond strengths than coatings produced by other processes. This is particularly useful when tough, resistant coatings, such as tungsten carbide, are required. The HVOF thermal spray process is basically the same as the combustion powder spray process except that this process has been developed to produce extremely high spray velocity. There are a number of HVOF guns that use different methods to achieve high velocity spraying. One method is basically a high pressure water cooled HVOF combustion chamber and long nozzle. Fuel (kerosene, acetylene, propylene and hydrogen) and oxygen are fed into the chamber, combustion produces a hot high pressure flame which is forced down a nozzle increasing its velocity. Powder may be fed axially into the HVOF combustion

chamber under high pressure or fed through the side of laval type nozzle where the pressure is lower. Another method uses a simpler system of a high pressure combustion nozzle and air cap. Fuel gas (propane, propylene or hydrogen) and oxygen are supplied at high pressure, combustion occurs outside the nozzle but within an air cap supplied with compressed air. The compressed air pinches and accelerates the flame and acts as a coolant for the HVOF gun. Powder is fed at high pressure axially from the center of the nozzle. The coatings produced by HVOF are similar to those produced by the detonation process. HVOF coatings are very dense, strong and show low residual tensile stress or in some cases compressive stress, which enable very much thicker coatings to be applied than previously possible with the other processes [11].

The very high kinetic energy of particles striking the substrate surface do not require the particles to be fully molten to form high quality HVOF coatings. This is certainly an advantage for the carbide cement type coatings and is where this process really excels. HVOF coatings are used in applications requiring the highest density and strength not found in most other thermal spray processes. New applications, previously not suitable for thermal spray coatings are becoming viable.

3.6 Experimental Design

The design of experiment is heavily used in the research. Experimental design methods have found broad application in many disciplines [12]. In fact, experimentation can be viewed as part of the scientific process and as one of the ways to reveal how systems or processes work. Experimental design is a critically important tool in engineering for improving the performance of a manufacturing process

Generally, the researchers could learn through a series of activities in which they make conjectures about a process, perform experiments to generate data from the process, and then use

the information from the experiments to establish new conjectures, which lead to new experiments, and so on.

Experimental design is a critically important tool in engineering world for improving the performance of a manufacturing process [12]. It also has extensive application in the development of new processes. The applications of experimental design techniques early in process development can result in: improved process yields, reduced variability and closer conformance to nominal or target requirements, reduced developmental time, and reduced overall cost.

Experimental design methods also play a major role in engineering design activities, where new products are developed and existing ones are improved. Some applications of experimental design in engineering design/process include:

1. Evaluation and comparison of basic design configurations.
2. Evaluation of material alternatives.
3. Selection of design parameters so that the product will work well under a wide variety of field conditions. Therefore, the product is robust.
4. Determination of key product design parameters that impact product performance.

Robust design is Dr. Taguchi's approach for determining the optimum configuration of design parameters for performance [13], quality, and cost. This method is to improve the implementation of total quality control. It is based on the design of experiments to provide near optimal quality characteristics for a specific objective. This method is often demeaned by academia for technical deficiencies, which can be improved by using response surface methodology. In the research, the design of experiments was used to conduct the ANOVA analysis and factorial design.

One of the proposed cleaning methods is ultrasonic peeling, which utilizes the high energy generated by ultrasonic vibration. Ultrasonic vibration physically moves the thermocouple horizontally or longitudinally under pressure. The energy created by the vibration should be sufficient to remove the condensate ash on the thermocouple tip. Some researchers have successfully applied the ultrasonic vibration to remove burrs from manufacturing process [14, 15]. In this research, burrs are defined as undesirable projections of material beyond the edge of a work piece during machining. Burrs are created around the edge of work piece due to plasticity during mechanical manufacturing process. Recently, because of miniaturization and increased precision of the machined parts, the size of burrs has been also reduced and deburring became even more difficult. Generally, burrs have been removed by method of physics and chemistry. There are a few publications in the area of applying ultrasonic to deburring [16-18]. When ultrasonic vibration propagates in the liquid medium, a large number of bubbles are formed. These bubbles generate an extremely strong force, which removes burrs [19]. The object of this study is to analyze the effects of ultrasonic vibration, medium and the type of abrasive in deburring process. From the above research, it is believed that peeling off the condensate ash shall require less energy than the burrs. Hence, we are confident that the ultrasonic vibration shall be a very successful solution to clean the thermocouple in gasifiers.

In our research, an ultrasonic welder was used to simulate the ultrasonic vibration to the thermocouple [20]. The vibration frequency was set to the range of 20 KHZ. The thermocouple probe was covered with cement-covered layers at the different thickness. These concrete layers were used to simulate the ash condensate in the gasifier. Different thickness was used to simulate the amount of ash condensate. The temperature changes were measured by the thermocouple of cement covered layers under the ultrasonic vibration applied environment.

The establishment of the coating on the surface will greatly improve the character of abrasion resistance, erosion resistance, heat resistance, chemical resistance regarding the part and the product. It can also give the character of the electric conductivity, insulation, and thermal conduction control.

The thermal spray coating process takes the energy from the inflammable gas, ionized gas, explosive gas, or electric energy, and heats the spray powder to a sufficient point (not necessarily to melting) whereby the feed stock will deform on impact [21]. It is propelled by the energy source gas stream at a target that the feed stock literally explodes onto the target, cools and forms a mechanical bond on the surface. Different heat sources determine the different spray processes [22]. Figure 1 illustrates the breakdown of different thermal spray processes. Basically, the thermal spray process includes the electric heat source and chemical (combustion) source due to the heat generation sources. The electric heat source includes plasma spray and wire arc spray. The plasma spray process is basically the spraying of molten or heat softened material onto a surface to provide a coating [23]. The wire Arc spray process uses the electric arc to melt a pair of electrically conductive wires. The molten material is atomized by compressed air and propelled towards the substrate surface. The chemical (combustion) heat source includes flame spray, high velocity oxygen fuel (HVOF) spray and detonation gun spray [24]. The flame spray and detonation gun basically consist of a long water cooled barrel with inlet valves for gases and powder. Oxygen and fuel (acetylene most common) are fed into the barrel along with a charge of powder [22,23].

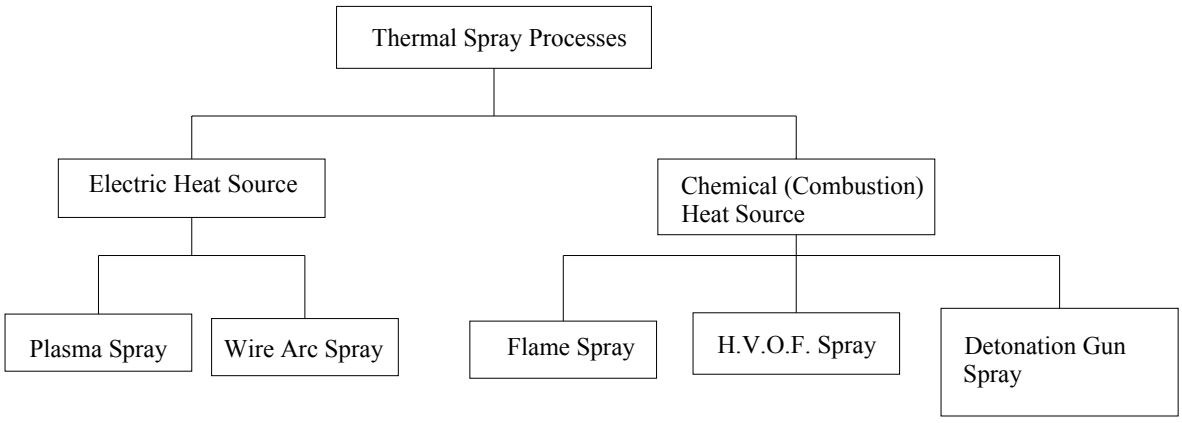

Figure 1. Schematic Flow Chart of the Different Thermal Spray Processes

The HVOF (high velocity oxygen fuel) thermal spray process is the same as the combustion powder spray process except that this process has been developed to produce an extremely high spray velocity. There are a number of HVOF guns that use different methods to achieve high velocity spraying [24]. One method is basically a high pressure water cooled combustion chamber and long nozzle. Fuels (kerosene, acetylene, propylene and hydrogen) and oxygen are fed into the chamber, and combustion process produces a hot high pressure flame which is forced down a nozzle increasing its velocity. Powder may be fed axially into the combustion chamber under high pressure or fed through the side of laval type nozzle where the pressure is lower. Another method uses a simpler system of a higher pressure combustion nozzle and air cap. Fuel gas (e.g. propane, propylene or hydrogen) and oxygen are supplied at high pressure. Combustion occurs outside the nozzle but within an air cap supplied with compressed air. The compressed air pinches and accelerates the flame and acts as a coolant for the gun. Powder is fed at high pressure axially from the center of the nozzle. Figure 2 shows the HVOC process.

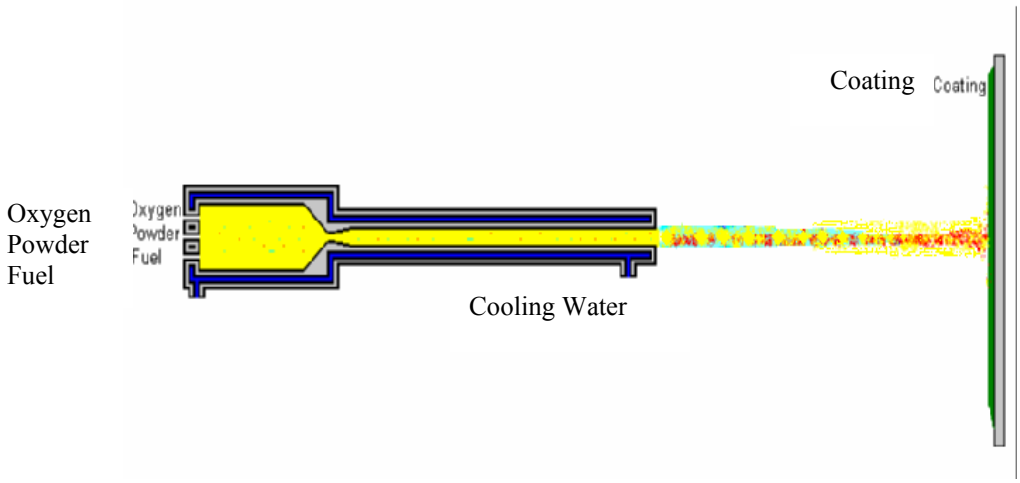

Figure 2 Schematic Diagram of the HVOF Process

The major advantage of HVOC process is that the coatings are very dense, strong and low residual tensile stress, which enable thicker coatings to be applied than the other processes.

The very high kinetic energy of particles striking the substrate surface does not require the particles to be fully molten to form high quality coatings. This is certainly an advantage for the carbide cermets type coatings and is where this process really excels [25]. HVOF coatings are used in applications requiring the highest density and strength not found in most other thermal spray processes. New applications, previously not suitable for thermal spray coatings are becoming viable.

HVOF spray technologies for application of tungsten carbide and chrome carbide based coatings have proved to be cleaner and more effective than chrome plating. Their superior performance is predicted to lead to significant reductions in life-cycle cost of ownership in industry. Development of Activated Combustion HVOF technology is expected to become a "break-through" in thermal spray applications for hard chrome replacement since this novel technology overcomes above-mentioned problems [26, 7].

The anti-erosion/corrosion coating sprayed on the thermocouple could make the thermocouple specialized and unique. The High Velocity Oxygen Flame (HVOF) coatings are used in applications requiring the highest density and strength not found in most other thermal spray processes [27]. HVOF Spraying is essentially a variation of powder flame spraying in which a modified torch is used to constrict the gas flow. HVOF coatings are usually denser and have higher bond strengths than coatings produced by other processes. This is particularly useful when tough, wear resistant coatings, such as tungsten carbide, are required. HVOF spray process ensures that the coating layer on the thermal couple tips are low-cost and reliable. Figure 3 shows the coated thermal couple via HVOF thermal spraying process, which is used for the experiment tests in this project.

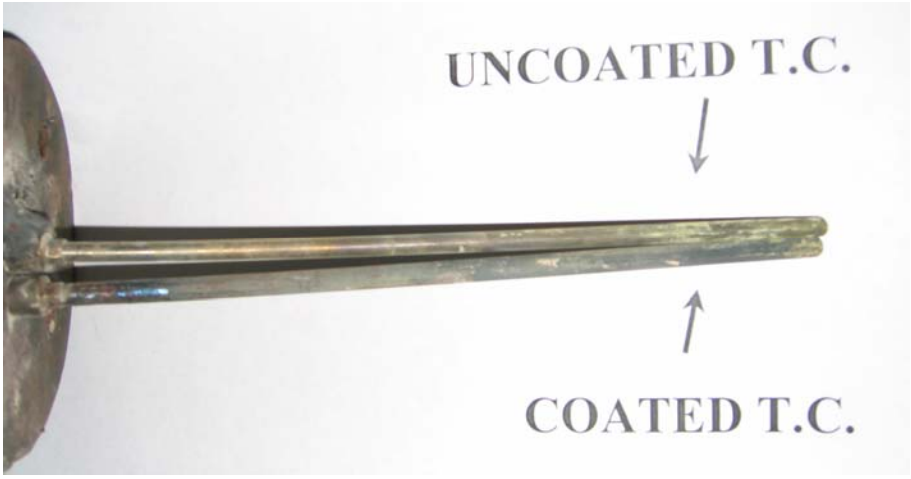

Figure 3 Pictorial view of Coated and Uncoated Thermal Couples

4. Design and Fabrication of the Gasifier Simulator

4.1 Gasifier Simulator Cold Model Design

The T-type thermocouple is used for cold model testing. A one (1) inch ID PVC tube is used as a sleeve to host the thermocouple. On top part of the sleeve, two ¼- inch holes were drilled to allow the compressed air to pass through. The thermocouple wire is connected to a DPi-32 temperature indicator. A DC power supply unit is used to supply the electric power to the thermocouple assembly. The schematic diagram of the thermocouple assembly is shown in Figure 4.

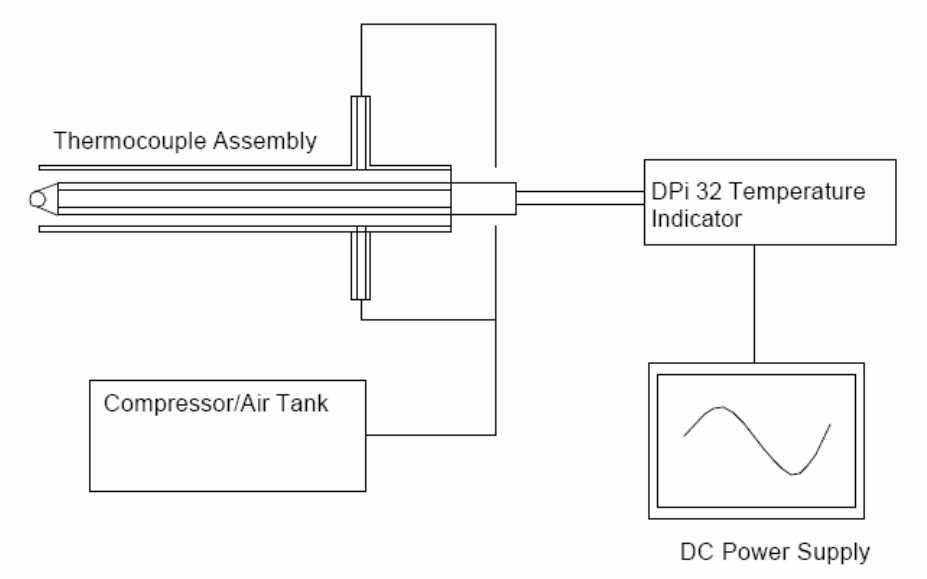

Figure 4 The Schematic Diagram of the Thermocouple Assembly for Cold Model Testes

The gasifier cold model for the project instrumentation was designed and fabricated. The cold model is made of an acrylic tube along with 10-inch ID and 20-inch of height. The tube is sealed with a pair of top flange and a pair of bottom flange. The top flange is designed with twenty (20) vent holes at ¼-inch of diameter. In addition, a one (1) inch hole was made to host the thermocouple assembly. The bottom flange is designed and fabricated with twenty (20) vent holes and four (4) irritating air injection holes. The irritating air injection holes are connected to

the controllable air blower. Two cloth filters are installed in both top and bottom flanges. The schematic diagram of the top and bottom flanges is shown in Figures 5 and 6.

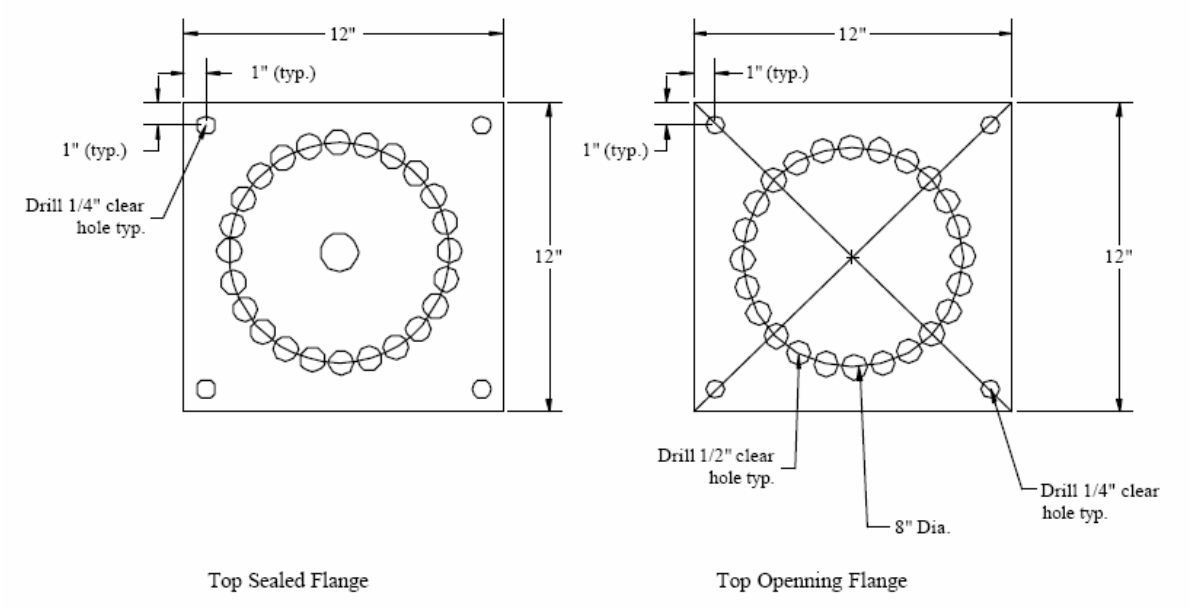

Figure 5 Design of the Top Flange for the Cold Test Model

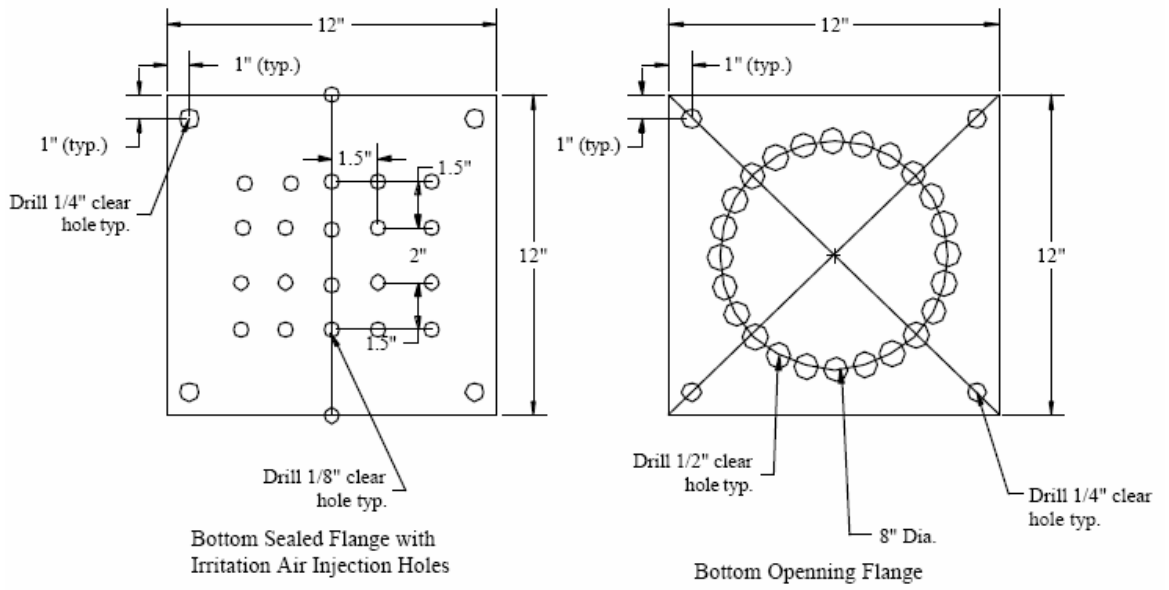

Figure 6 Design of the Bottom Flange for the Cold Test Model

4.2 Gasifier Simulator Hot Model Design

4.2.1 Gasifier Chamber Design

The gasifier simulator (hot model) chamber is made of carbon steel pipe of 24-inch high and the outside diameter is 8-inch. The thickness is 0.25-inch as shown in Figure 7. The electric heating coil was installed inside the gasifier chamber. The electric heating oil is made from Mor Electric Heating Assoc., Inc. The main component of the heating coil is L17-10C nichrome wire coil which can heat the inside material up to 1200 ^{o}C with 3 kW of inputted electric power. The wire coil is held and insulated from the conducting gasifier wall using the ceramic insulator built in the refractory layer. The operating temperature will be maintained at the range of 800-1200 ^{o}C for the experiment. The refractory layer was attached to the inner side of the chamber wall to maintain relative high temperature which can simulate the real gasification environment. A certain amount of bars were welded to the wall to hold the refractory layer. The boiler refractory cement was used as the refractory material. The heat conduction coefficient is 0.8 w/(m $_{o}$C). The small amount of heat will be transferred to the outside, which can keep the inside temperature at relatively steady state. The refractory layer thickness is determined by the following equation [1].

$$d2/d1=\exp(2*\pi*\lambda*(T1-T2)/Q)$$

where d1 and d2 are the inner and outer diameter of the refractory layer, λ is the heat conduction coefficient of the refractory material, T1 and T2 are the inner and outer side temperature of the refractory layer, respectively, and Q is the heat transfer by conducting.

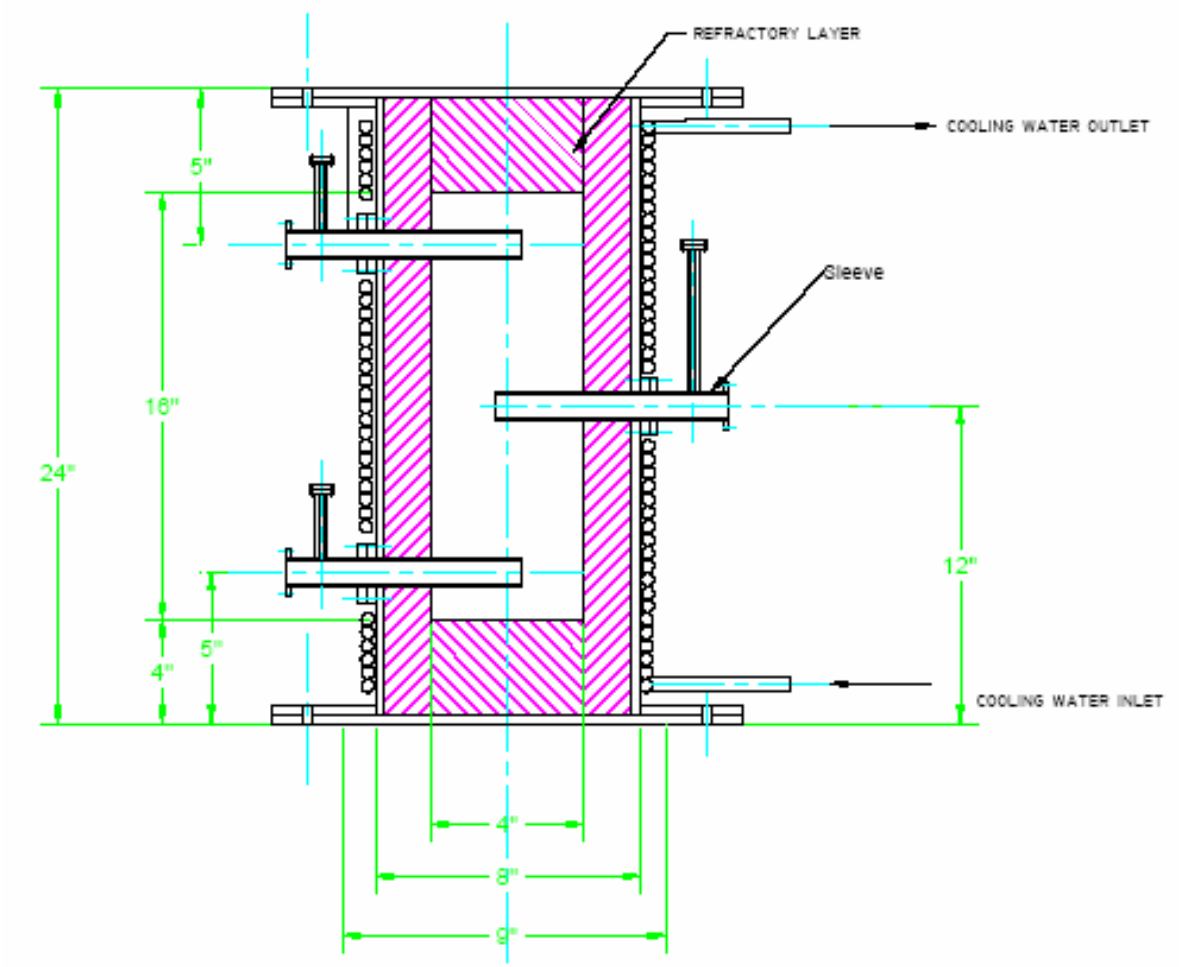

Figure 7. The Schematic Diagram of the Proposed Gasifier Simulator (hot model)

In order to compare the temperature at different locations, three (3) temperature measurement holes are drilled with a diameter of 1 1.25-inch as also shown in Figure 7. A short pipe with diameter of 1.25-inch and thickness of 0.125-inch is welded to the hole. At the end of the pipe, a flange is welded to connect the sleeve. Two couples of flanges were welded at the upper and bottom end of the chamber to seal the gasifier simulator (hot model). Two holes are drilled for the electric heating coil in the upper blind flange.

4.2.2 Heat Exchanger Design

The water heat exchangers were made of copper coil of 0.25-inch diameter. The copper coil was wired to the outer side of the chamber. Cooling water is pumped through the copper coil

and the high speed water could carry out the heat to keep the outer surface temperature down (around 110 degree F). This type of heat exchanger maintains high efficiency because of high heat conduction materials and high fluid flow rate. The water flow rate is controlled through a water temperature monitor.

4.2.3 Thermocouple Sleeve Design

The thermocouple probe sleeve is designed as shown in Figure 8. The sleeve tube is 0.75-inch inner diameter with 0.125-inch thick and 7-inch long. A flange is welded to the end of the tube. The probe is fixed at the center of the sleeve. Another tube with the same size is welded vertically to the sleeve. The cooling air is introduced through this pipe periodically to reduce the sleeve temperature. The sleeve is made of stainless steel which can stand very high temperature.

4.2.4 Fabrication of the Gasifier Simulator (Hot Model)

The details of the gasifier simulator (hot model) were carefully designed for the fabrication. The gasifier simulator (hot model) chamber, the thermocouple sleeves, and accessories including flanges, insulation layers, heat exchangers were fabricated carefully based on the detailed designs, which was collaborated by the private fabrication company- K&C Welding & Construction. Morgan research laboratory staff has worked closely with the fabrication company for the assurance of the fabrication quality. The Figures 9-11 show the pictorial view of the gasifier simulator (hot model), the sleeve and the thermocouple.

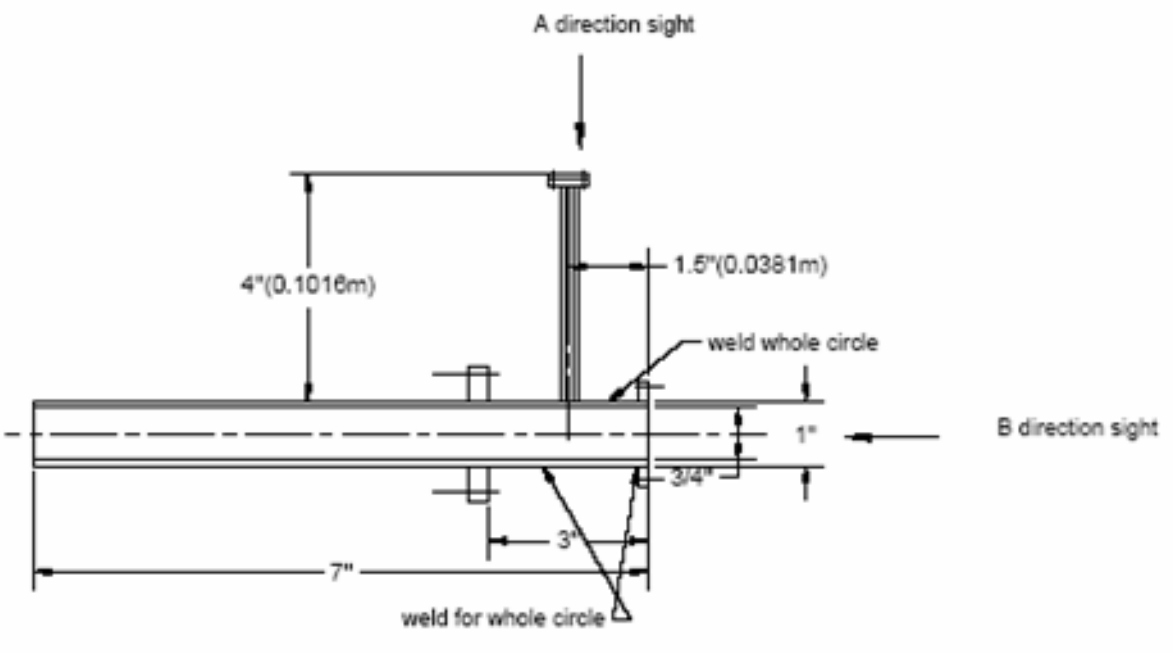

Figure 8 The Schematic Diagram of the thermocouple Sleeve

Figure 9 The Sleeve for the Gasifier Simulator(Hot Model)

Figure 10 The Gasifier Simulator (Hot Model) Test Facilities

Figure 11 The Thermocouple Probe (K-Type) for Gasifier Simulator (Hot Model)

4.3 Facilities for Ultrasonic Vibration Application Experiments

The ultrasonic vibration system was manufactured in Sonobond Ultrasonics Company [28]. The pictorial view of the system is shown in Figure 12. The ultrasonic welder is composed of a hand held device and a generator. The hand held device consists of a handle, trigger switch, converter, horn and name plate on the handle. While the generator (model name – RL35) consists of a generator module handle, model designation, LED (light emitting diodes) bar, LED power, function key "US-TEST" (ultrasonic test), weld time, hold time, fastening screws, mains switch and status displays [28]:

- US ON (green)
- Valve (green)
- Error (red)

In making one more familiar to the ultrasonic device, it is necessary to comprehend the actual size of the generator, this includes:

- Width = 130mm
- Length = 450mm
- Height = 300mm
- Weight = 7kg

Figure 12 Pictorial View of Ultrasonic Vibration Testing Facility

The experiments are conducted by the following the procedure:

1. Prepare the covered specimen of thermocouple.
2. Set up the gasification environment parameters.
3. Turn on the cooling water to keep the outer wall of gasifier in lower temperature.
4. Install the clean thermocouple into the gasifier.
5. Switch on the heating coil and start the heating process.

6. Start recording the temperature data
7. Connect the thermocouple probe to the specimen once the temperature reaches the steady state and keep recording the temperature data.
8. Apply the ultrasonic vibration continuously once the new temperature reaches the steady state.
9. Observe closely and record the temperature changes during the ultrasonic vibration application.
10. Turn off the heating coil and start the shutting down procedure.

5 Experimental

5.1 Cold Model Experimental

5.1.1 Experimental and Operational Data

The shakedown test of the cold model was conducted in the Center for Advanced Energy Systems & Environmental Control Technologies at Morgan State University. The shakedown tests could determine the sealing performance, air circulation and filter performance for the cold model design. In order to the conduct effective cold model tests, the air leak between each flange is not allowed because of the dirty environment inside the cold model. The air should go through the filter and then vent to the atmosphere. The major experimental and operational data are included in the report.

5.1.1.1 Air Leaking Test

Eleven (11) tests were conducted to check the air leak in the cold model system. The voltage regulator was used to control the blower to provide different air flow rates for the cold model. During the tests, the measured parameters were voltage regulator's reading and pressure difference delta P. The air velocity and the air flow rate were the calculated parameters based on the recorded data.

5.1.1.2 Air Circulations and Filter Performance Testing

Similarly, eleven (11) tests were conducted to determine the air circulation and filter performance. In each test, the air flow was following the path which is what we expected; Air blower –cold Model – vent holes – filter – atmosphere.

5.1.1.3 Temperature Influence Testing by Electric Motor

In order to get the basic temperature measurement behavior in the cold model, a series of temperature measurement shall be conducted under an ambient temperature condition before the

cold model tests are conducted. Since an electric air blower is used in the cold model testing system, the influence of the electric motor to the temperature inside the cold model shall be evaluated. Six (6) tests were conducted to determine at what test condition the electric motor has the least influence to the temperature inside the cold model. The T-type thermocouple and the DPi-32 temperature indicating system require several minutes of warming up time. Hence, ten (10) minutes warming up time was given for each test at different voltage settings. The time interval between each temperature reading was one (1) minute.

5.1.1.4 Cold Model Systematic Test

As a continuation of the last semi-annual report, the gasifier simulator (cold model) testing parameters were set in the following settings. All together four (4) parameters are being tested at mixed levels shown in Table 1. Hence, thirty-two (32) cold model tests have been conducted.

The cold model testing parameters can be set in the following settings. All together four (4) parameters are being tested at three (3) different levels. Hence, sixty-four (64) cold model tests will be conducted. Table 1 shows the list of the test parameters and the level design.

The cold model met the design requirement and was ready for the systematic testing. The detailed experimental procedure is shown as follows. 1) Assemble the gasifier simulator (cold model), blower, manometer, and filter together. 2) Put certain amount of filtered sawdust on the distributor plate. 3) Calibration of the manometer and electronic scale. 4) Set the gasifier simulator (cold model) into different cases for testing. 5) Operate the voltage regulator to obtain the different experimental conditions. 6) Record the experimental temperature data.

The ultrasonic attachment used in the gasifier simulator (cold model) systematic test was a 40kHz transducer, which was driven by 120 volts electric power. The transducers were mounted

on the sleeve. The transducer face was pointed to the thermocouple tip with 0.25-inch distance. The ultrasonic implementation for the gasifier simulator (cold model) systematic tests was an air application, which meant that the air would be the medium to transport the ultrasound.

Table 1.Test Parameters and the Level Design for Cold Model Tests

Parameter 1	
Irritation air flow rate:	
Level 1:	0.0141 m3/s
Level 2:	0.0200 m3/s
Level 3:	0.0253 m3/s
Parameter 2	
Compressed air injection frequency	
Level 1:	1/120 hz
Level 2:	1/60 hz
Level 3:	1/30 hz
Parameter 3	
Weight of the simulated dust	
Level 1:	200 grams
Level 2:	400 grams
Level 3:	600 grams
Parameter 4	
Ultrasound Application	
Level 1:	No
Level 2:	1 device
Level 3:	2 devices

5.1.2 Results and Discussion

From Tables 1, no air leak was recorded in the cold model under the cold model testing. The air flow in the cold model operation is also following the path we expected, which is air blower – cold model – vent holes – filter – atmosphere. From the temperature influence testing by electric motor, temperature in the cold model increased along with the time increasing. The slope increased when voltage percentage increased. Figure 13 shows the details of the temperature measurements.

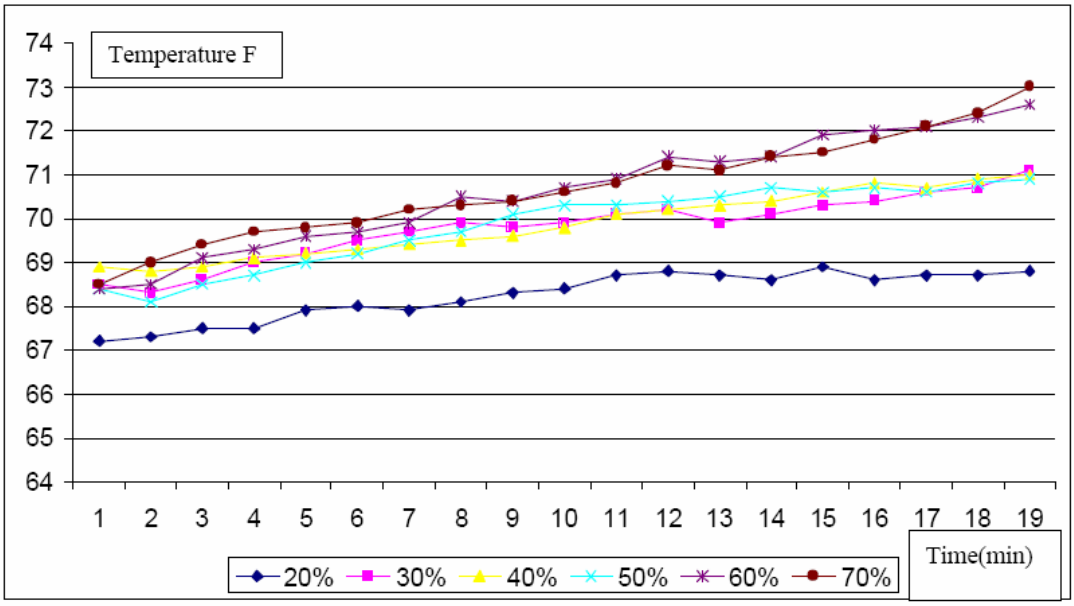

Figure 13 Temperature Behaviors in Cold Model at Different Voltage Settings

At 20% voltage, the transient temperature deviated from the other group. At 30%, 40% and 50% voltage, the transient temperature increased at lower slope in comparing with that of 60% and 70% voltage.

The detailed gasifier simulator (cold model) testing data are shown in the Figure 14-37 in appendix. Our previous system test revealed that the temperature readings at dirty dust environment differed from the sample curve at clean environment. Figures 14-22 show the temperature curves at the following experimental conditions- 200 grams of dust particles. Figures 14-16 show the temperature curve without ultrasonic application. The temperature reading at 1 min, 2 min, and 0.5 min injection intervals fluctuated over the sample temperature curve at the clean environment.

This result indicated that the air injection did clean the thermocouple tip. From Figures 14-16, it can be seen that the airflow rate did not have the clear trend of changing fluctuations. Figures 17-19 show the temperature curve with one (1) ultrasonic application. Figures 17-19 show similar result of Figures 14-16. It is believed that one (1) ultrasonic air application does not

have significant impact on the temperature readings. Figures 20-22 show the temperature curve with two (2) ultrasonic applications. Figures 20-22 indicate that two (2) ultrasonic air applications may not have significant impact on the temperature readings. Figures 23-27 show the repeatability of the tests.

Overall temperature curves matched each other pretty well. This indicates the repeatability of the gasifier simulator (cold model) systematic tests. Figures 29-37 show the temperature curves at the following experimental conditions- 400 grams of dust particles. All the curves seem similar to the curves in Figures 27-35. Among Figures 29-37, Figures 29-31 show the temperature curve with no ultrasonic application. Figures 32-34 show the temperature curve with one (1) ultrasonic application. Figures 35-37 show the temperature curve with two (2) ultrasonic applications. From Figures 14-37, it can be seen that the air injection cleaning method did have positive impact to bring the differed temperature back to the clean sample. By comparing the curves, one (1) minute injection interval had the best performance for the accurate temperature measurement.

The result also indicates that the dust amount in the gasifier simulator (hot model) did not affect the temperature.

5.1. 3 Data Analysis and Modeling on Gasifier Simulator (Cold Model) Testing

5.1. 3.1 ANOVA/Regression Analysis on Gasifier Simulator (Cold Model) Testing

Due to the heat generated by the electric motor, the temperature increased with the time. This temperature increment was used to evaluate the impacts of the experimental parameters. The temperature measurement data in the gasifier simulator (cold model) testing are shown in the Appendix A. All the data were inputted to the Minitab for analysis. Basically, for the Analysis of Variances (ANOVA), five (5) factors were considered as the significant factors that can affect the temperature reading in the gasifier simulator (cold model). These five (5) factors are time(t),

dust particle amount (DP_{amount}), number of ultrasonic applications (N_{ultra}), air flow rate (F_{air}), and injection time intervals ($It_{intervals}$). DP_{amount}, N_{ultra}, F_{air}, and $It_{intervals}$ levels design are listed in the above Table 1. The level design of the time is shown below.

Time (t): Nineteen (19) levels

Level 1: 1 min; Level 2: 2 min; Level 3: 3 min; Level 4: 4 min; Level 5: 5 min; Level 6: 6 min Level 7: 7 min; Level 8: 8 min; Level 9: 9 min; Level 10: 10 min; Level 11: 11 min; Level 12: 12 min; Level 13: 13 min; Level 14: 14 min; Level 15: 15 min; Level 16: 16 min; Level 17: 17 min; Level 18: 18 min; Level 19: 19 min

ANOVA Analysis:

The analysis was conducted on two cases, without normalized room temperature and with normalized room temperature.

Case 1: Without Normalized Room Temperature

One-way Analysis of Variance was conducted on all five (5) parameters respectively. The results showed that all five (5) factors have significant impact on the temperature reading in the gasifiers. Among these factors, time (t) has the most significant impact on the temperature reading. The ultrasonic application has the second significant the impact on the temperature reading. Air flow rate has the third significant impact on the temperature reading. The dust particle weight has the fourth significant impact on the temperature reading. The injection time interval has the least significant impact on the temperature reading.

The general linear model analysis was also conducted to determine if any correlation among the factors. No obvious coloration was found since the results for each factor are similar to the one-way ANOVA.

Case 2: With Normalized Room Temperature

Similar results were found in the ANOVA with normalized room temperature. All five (5) factors were found all significant for the temperature reading. The sequence was also similar to the ANOVA without the normalized room temperature.

5.1.3.2. Linear Regression Analysis on Gasifier Simulator (Cold Model) Testing

The regression analysis was conducted on two cases, without the normalized room temperature and with the normalized room temperature.

Case 1: With Normalized Room Temperature

The regression equation for the temperature reading in the gasifier simulator (cold model) under normalized room temperature is shown in equation (1).

Temp. Readings = 67.2 + 0.126 * (Time) + 0.0746 * (Ultrasonic) + 0.128 * (Injection Intervals) + 0.0213 * (Airflow Rate) -0.000366 * (Dust Particles) (1)

The statistical results of the linear regression process with normalized room temperature are shown in Table 2.

Table 2. Statistical Output of the Linear Regression Process with Normalized Room Temperature

Predictor	Coef	StDev	T	P
Constant	67.1847	0.0636	1055.58	0.000
Time	0.125692	0.001904	66.00	0.000
Ultrasou	0.07456	0.01278	5.84	0.000
Injectio	0.12807	0.01673	7.66	0.000
Airflow	0.021295	0.001082	19.68	0.000
Dust Par	-0.0003665	0.0001043	-3.51	0.000
S = 0.3341	R-Sq = 82.6%	R-Sq(adj) = 82.5%		

5.2 Hot Model Tests

5.2.1 Temperature Changes under Various Environments

5.2.1.1 Temperature Changes under Air Supply Environment

The data for temperature changes under air environment experiment is shown in Table A-1 in Appendix II. Temperature changes under the air injection condition are shown in Figure 14. The temperature inside the gasifier changed smoothly during the heating up process. Once the temperature reaches the steady state, the thermocouple was exchanged with the cement-covered one. As shown in Figure 14, the temperature was dropped sharply at that moment. At that point, the temperature was measured using the covered thermocouple. Once the measured temperature reached steady state, the ultrasonic vibration was applied. The temperature slightly decreased due to the cooling process applied to the ultrasonic vibration. Then the temperature increased steadily. This phenomenon means that the ultrasonic vibration could shake away the cement cover.

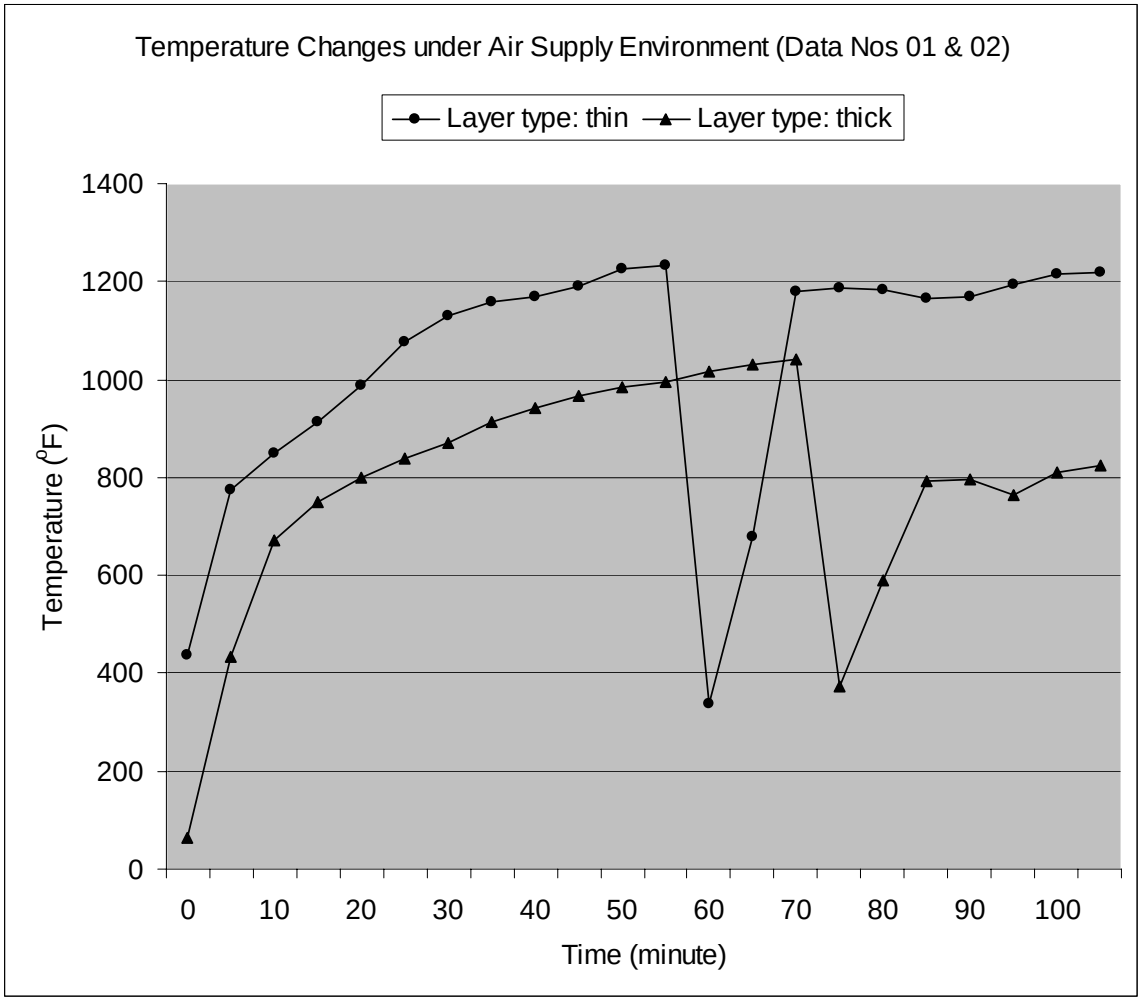

Figure 14 Temperature Changes under the Air Supply Environment

5.2.2 Temperature Changes under Air/Water Supply Environment

The temperature changes under air and water supply environment were tested and the data are shown in Table A-1 in Appendix II. Figure 15 shows the experimental results under the air and water environment. The thermocouple specimens were the same size as in the only air environment case. The experiments under this environment were repeated once for each thermocouple specimen of the cement-covered layer. The temperature changed smoothly at the heating up process. The thermocouple by the cement-covered layer caused the steady state

temperature gap. After application of ultrasonic vibration, the temperature slightly decreased and then reached the steady state.

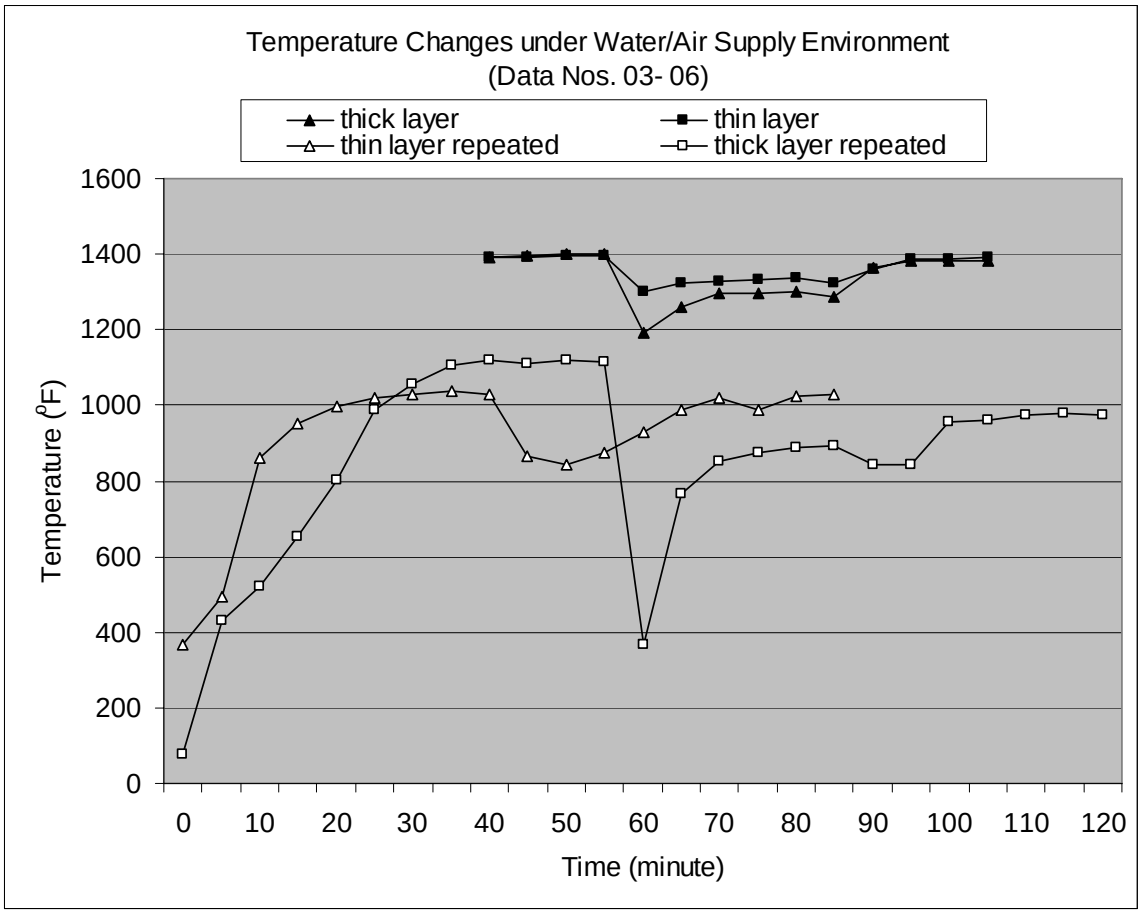

Figure 15 Temperature Changes under Air and Water Supply Environment

5.2.3 Temperature Change under Air/Water/Ammonia Environment

The experiments regarding to the air, water and ammonia environment were conducted to examine the temperature changes. The data of temperature change are shown in Table A-2 in Appendix II. The temperature changes are shown in Figure 16. The thin and thick cement-covered thermocouples were used in these experiments. The experiments were repeated two times for each environment. The temperature changes followed the similar trend as previous

cases. The temperature changes after the application of ultrasonic vibration decreased slightly and then reached the steady state.

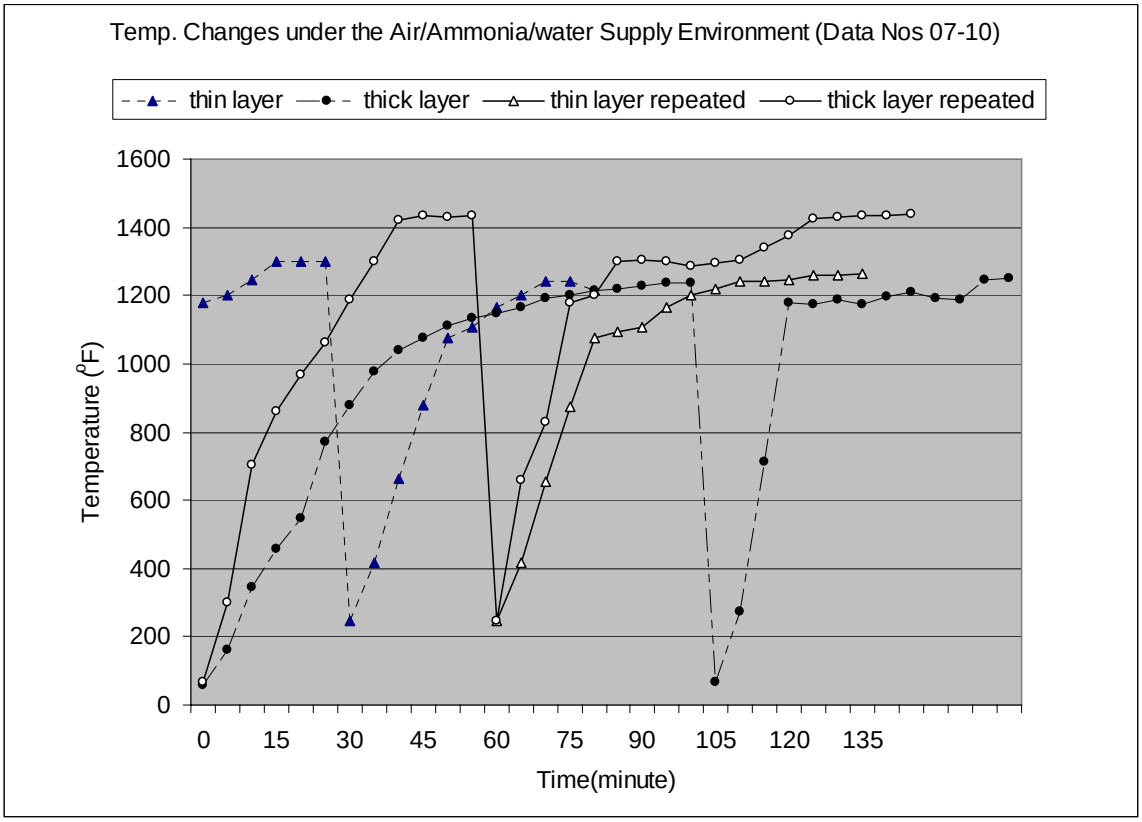

Figure 16 Temperature Changes under the Environment of Air/Water/Ammonia Supply

5.2.4 Temperature Changes under the Environment of Air/Water/Ammonia/Fine Dust Supply

The temperature changes under the all combined factors were conducted and the data are shown in Table A-2 in Appendix II. The amount of fine dust particles was 75 grams with the particles size of 0-250 μm. The fine dust particles were pre-injected into the gasifier. The temperature changes under this environment are shown in Figure 17. The temperature is not smoothly changed during the heating up process (time period from beginning to 140 minutes). It is believed that the dust particles were heated and the unburned carbon caused the unstable temperature status. After the heating up process, the temperature changes were maintained as

steady state. The ultrasonic vibration was then applied to the thermocouple probe. The temperature changes are similar in patterns with the other cases (in Section 5.1-5.3).

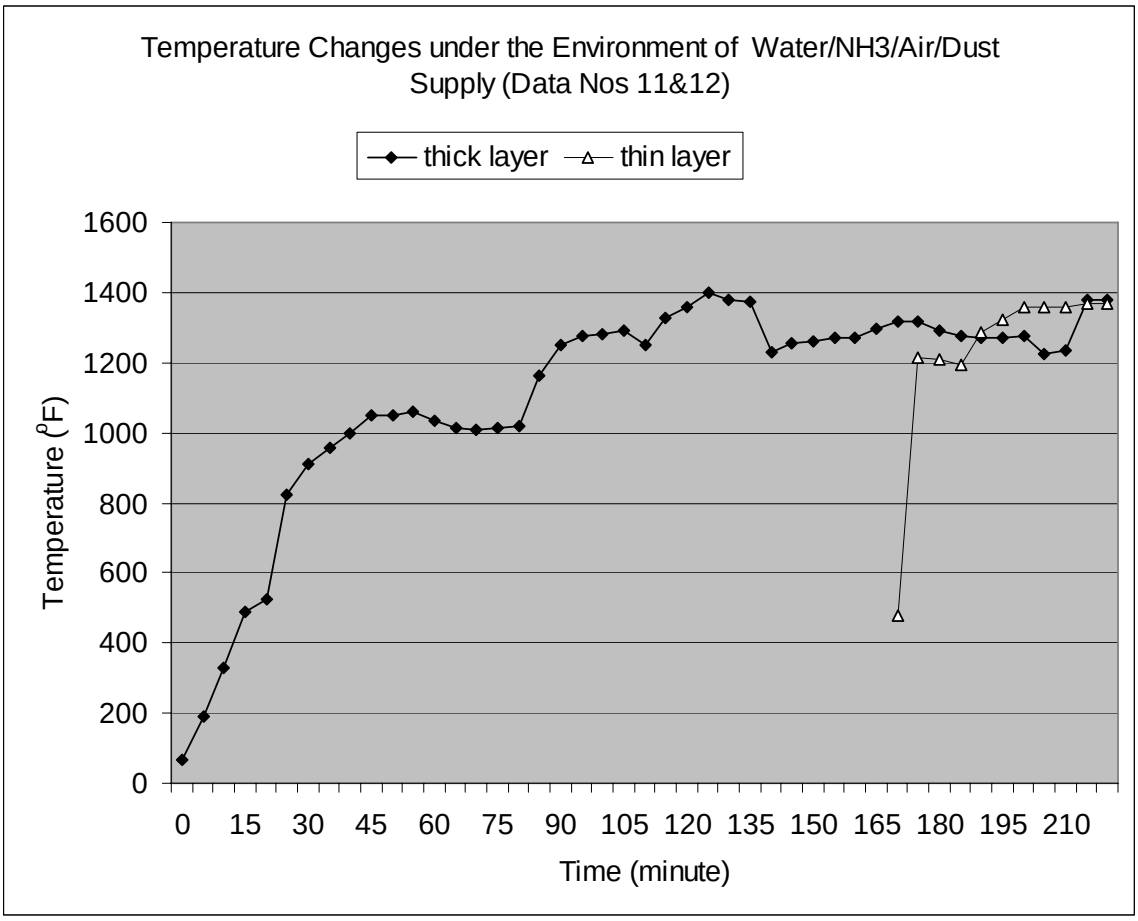

Figure 17 Temperature Changes under the Environment of Air, Water, Ammonia and Fine Dust Particles Supply

5.2.5 Analysis of Experimental Data & Results under Hot Temperature Condition

In order to examine the effects of input factors on the temperature changes inside the gasifier, the analysis of variance (ANOVA) method was applied [29]. The input factors include different combinations of environments under air, water, ammonia, and dust, and the thickness of covered cements. The response variable was temperature. The detailed data for input factors and response variable are shown in Table 3.

Using statistical software SPSS 12.0, the analysis of variances of temperature is shown in Table 4. From the Table, the input factors do not show significant effects to the temperature changes inside the gasifier at the type-I error of 0.1.

Table 3 Hot Model Test Results of the Ultrasonic Vibration Application

Air (m3/sec)	Water (ml/sec)	Ammonia (ml/sec)	Thickness (mm)	Dust (gram)	Temp. (F)
0.0032	0	0	6.7	0	1218.5
0.0032	0	0	12.8	0	825.6
0.0032	0.0033	0	6.7	0	1387.3
0.0032	0.0033	0	12.8	0	1383
0.0032	0.0033	0	6.7	0	1026
0.0032	0.0033	0	12.8	0	977.77
0.0032	0.0033	0.003	6.7	0	1240.5
0.0032	0.0033	0.003	12.8	0	1248
0.0032	0.0033	0.003	6.7	0	946.5
0.0032	0.0033	0.003	12.8	0	1435.25
0.0032	0.0033	0.003	6.7	75	1362.8
0.0032	0.0033	0.003	12.8	75	1379.5

Table 4 ANOVA Table for the Ultrasonic Vibration Application

Parameter	Unstandardized Coefficients		Standardized Coefficients	t	Significance level
(Constant)	1004.06	258.965		3.877	.006
Air	/	/	/	/	/
Water	51959.85	58456.84	.323	.889	.404
Ammonia	8015.000	52502.79	.061	.153	.883
Thickness	1.845	21.083	.028	.088	.933
Dust	2.048	2.572	.289	.796	.452

5.3 Data Acquisition System

5.3.1 Design of DAS

The OMB-DAQ-54 Data Acquisition System (DAS) is used to record the temperature measurement accurately and automatically. The OMB-DAQ-54 Data Acquisition System (DAS) is attached to the whole gasification simulator. The OMB-DAQ-54 Data Acquisition System

(DAS) is a full-featured data acquisition product that utilizes the Universal Serial Bus (USB), which is built into almost every new personal computer. Designed for high accuracy and resolution, the 22-bit OMB-DAQ-54 data acquisition systems directly measure multiple channels of thermocouple, voltage, pulse, frequency. A single cable to the PC provides high-speed communication and power to the OMB-DAQ-54. The OMB-DAQ-54 avoids many of the limitations of PC-Card (PCMCIA) data acquisition devices and offer advantages over many PC plug-in data acquisition boards as well [30].

The OMB-DAQ-54 data acquisition system offers ten single-ended or five (5) differential analog (up to ±20 V full scale) or thermocouple input channels with 16 programmable ranges and 500 V optical isolation as shown in Figure 18. To simplify attachment of signals and transducers, the OMB-DAQ-54 modules feature convenient, removable screw-terminal input connections.

Personal DaqView allows the creation of real-time displays using built-in display options, including digital, dial meter, bar graph, and strip chart displays. Thermocouple type and temperature ranges: K (-200 to 1200°C), and thermocouple accuracy: K (±1.2°C). Figure 18 shows the pictorial view of the OMB-DAQ-54 module.

The schematic diagram of the whole gasification simulator system with the temperature data acquisition subsystem is shown in Figure 19. The coated and uncoated thermal couples are connected directly to the OMB-DAQ-54 module. Two out of five provided channels are used for the temperature measurement. The module is connected to a personal computer through a universal series bus (USB). The pictorial view of the whole system is illustrated in Figure 20.

Figure 18 Pictorial View of OMB-DAQ-54 Data Acquisition Module

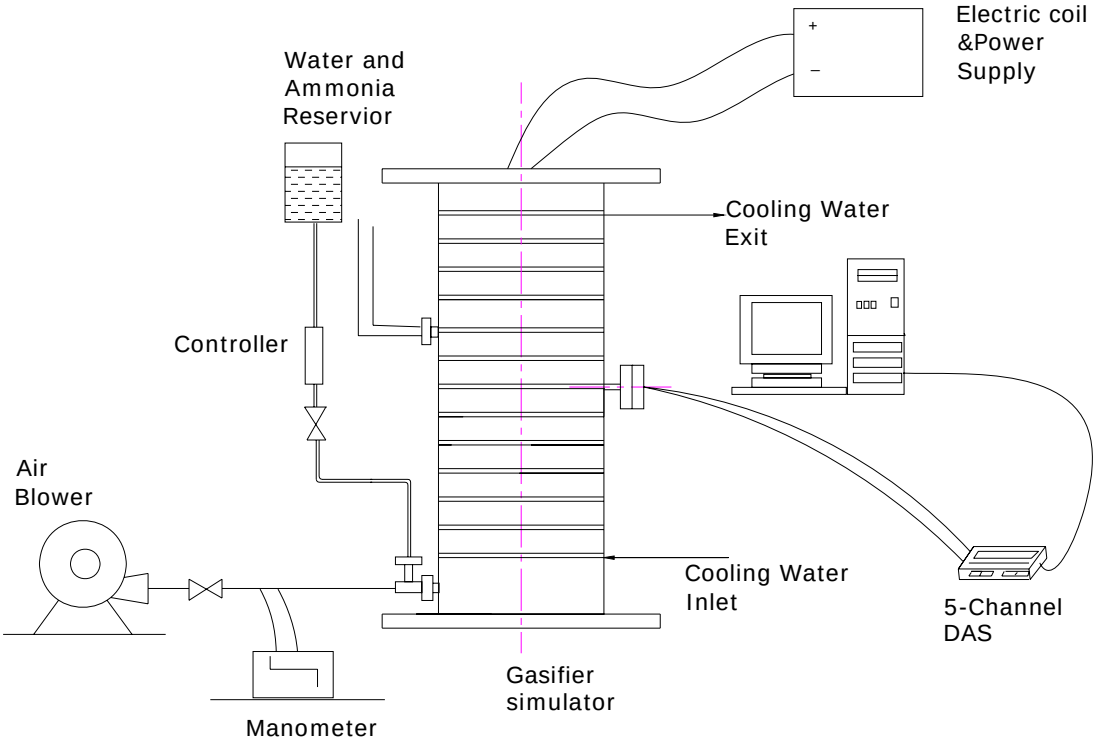

Figure 19 Schematic Diagram of Gasification System with 5-channel DAS

Figure 20 Pictorial View of the Gasifier Simulation System with 5-channel DAS

The Personal DaqView with the associated authorization code is the attached software for the OMB-DAQ-54 module. The Personal DaqView is window-based software which can be installed in Microsoft Windows 98SE/WindowsME/2000 or XP. Figure 21 is an illustration of 5-channel DAS and DaqView interfaces.

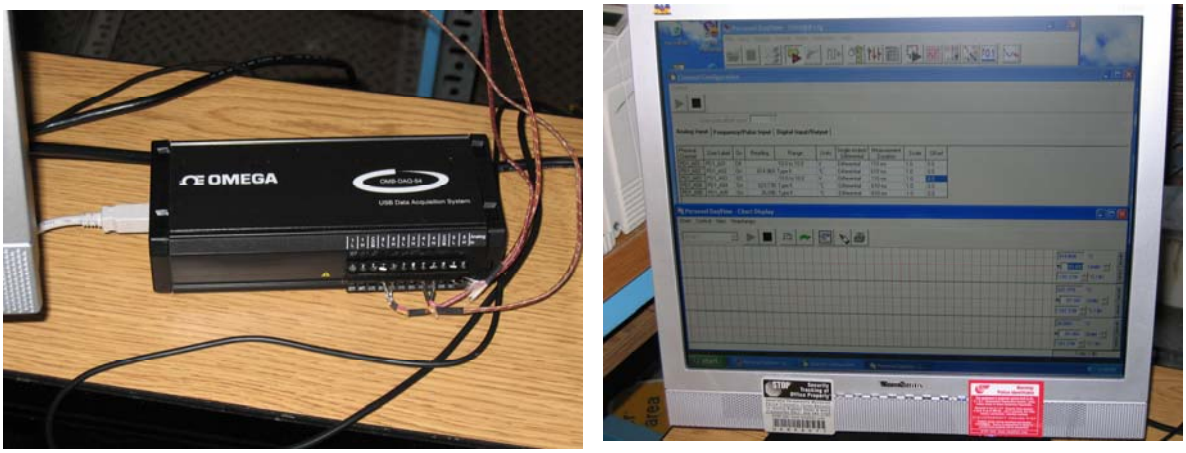

Figure 21 Pictorial View of 5-channel DAS and Personal DaqView

5.4 Effect of Coating on Temperature Measurements

5.4.1 Effects of the Coated Thermal Couple on the Temperature Measurements

The temperature readings of coated and uncoated thermal couples are identical throughout the test period as shown in Figure 22. The temperature for uncoated thermal couple is uniformly higher than that of the coated thermal couple. The average temperature difference is 8.7 ^{o}C for this condition.

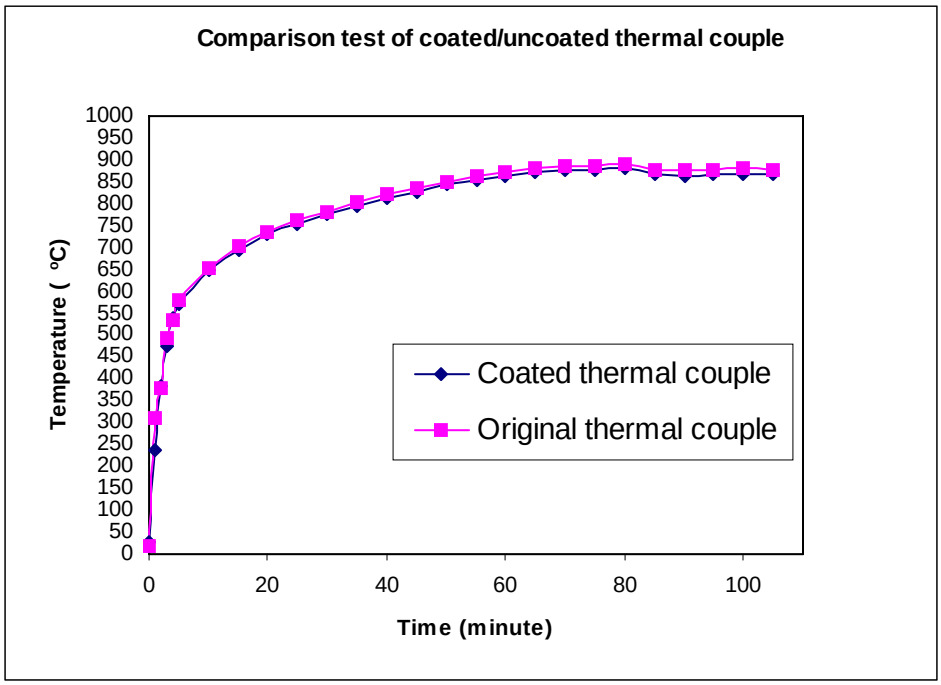

Figure 22 Comparison Tests on Temperature Measurement for Coated/Uncoated Thermocouples

Figure 23 shows the comparison test of coated and uncoated thermal couples under the condition: 10 voltages for air flow, 2 ml/min for ammonia & water, and 75 gram for fine dust particles. The temperature changes indicate identical temperature readings for coated and uncoated thermal couples throughout the testing. The temperature for uncoated thermal couple is uniformly higher than that of the coated thermal couple. The average temperature difference is 15.4 ^{o}C for this condition. It is believed that the coating layer will increase the heat resistance

between the thermal couple tip and the object. The increased heat resistance affects the temperature difference.

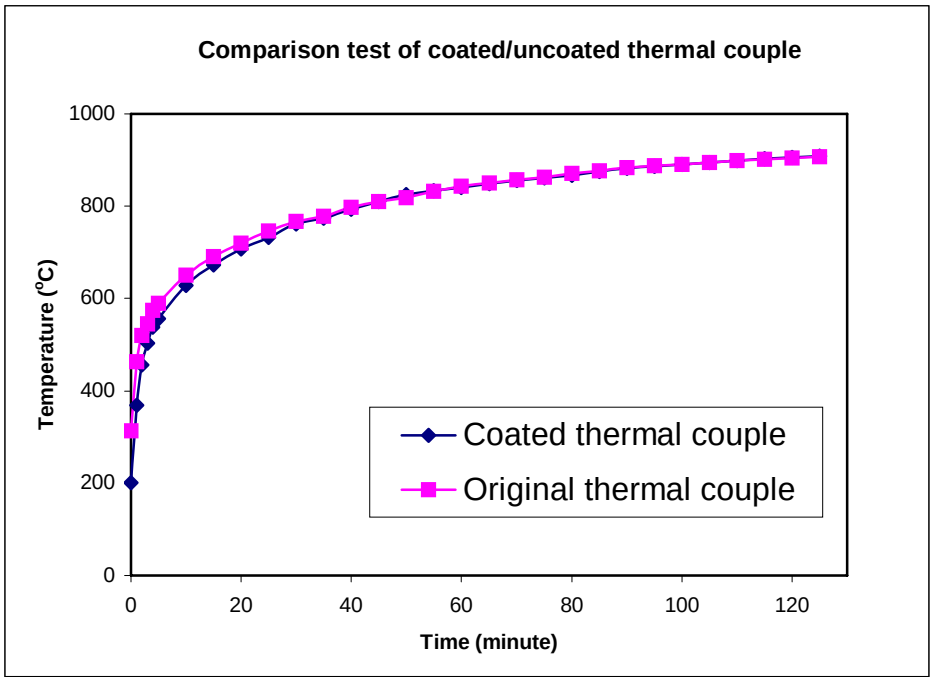

Figure 23 Comparison Tests on Temperature Measurement for Coated/Uncoated Thermocouples

Figure 24 shows the comparison test of coated and uncoated thermal couples under the condition: 15 voltages for air flow, 3 ml/min for ammonia & water, and 75 gram for fine dust particles. The temperature plots also show the identical distribution of the temperature readings for coated and uncoated thermal couples throughout the testing. The temperature for uncoated thermal couple is uniformly higher than the temperature for coated thermal couple. The average temperature difference is 9.4 ^{o}C for this condition.

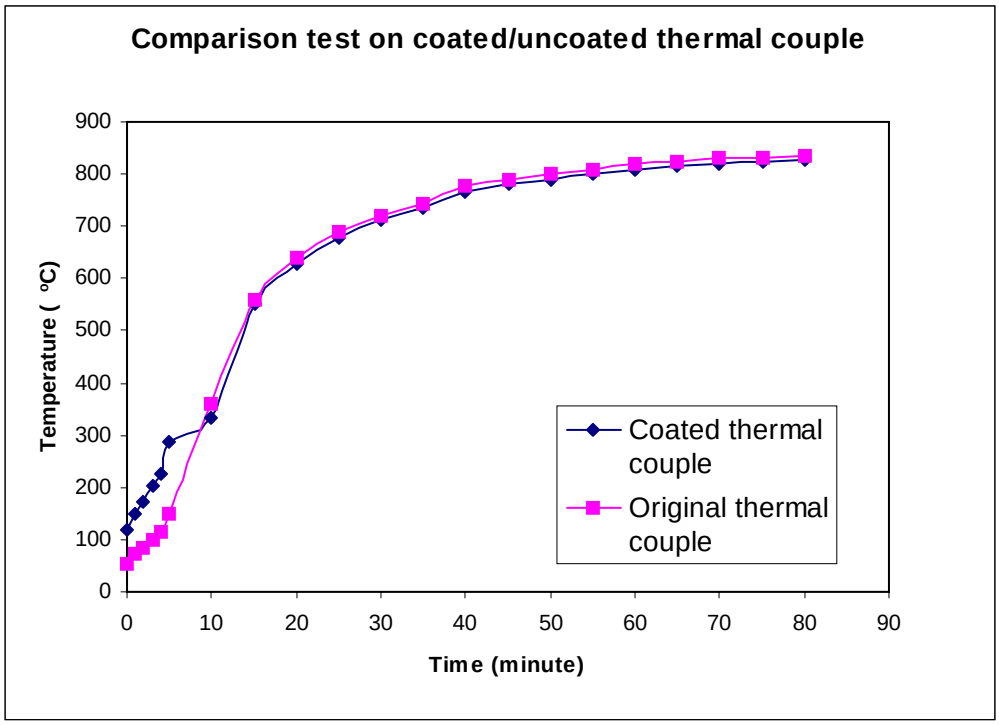

Figure 24 Comparison Tests on Temperature Measurement for Coated/Uncoated Thermocouples

After the installation of data acquisition system (DAS), additional experiments are continued as shown in Table 1. The details of the temperature changes are attached in Appendix 2.

Figure 25 shows the comparison test of coated and uncoated thermal couples under the condition: 10 voltages for air flow, 3 ml/min for ammonia & water, and 75 gram for fine dust particles. The temperature plots also show the identical of the temperature readings for coated and uncoated thermal couples throughout the testing time interval. The temperature changes for uncoated thermal couple are uniformly higher than that o the coated thermal couple. The average temperature difference is 23.2 C for this condition.

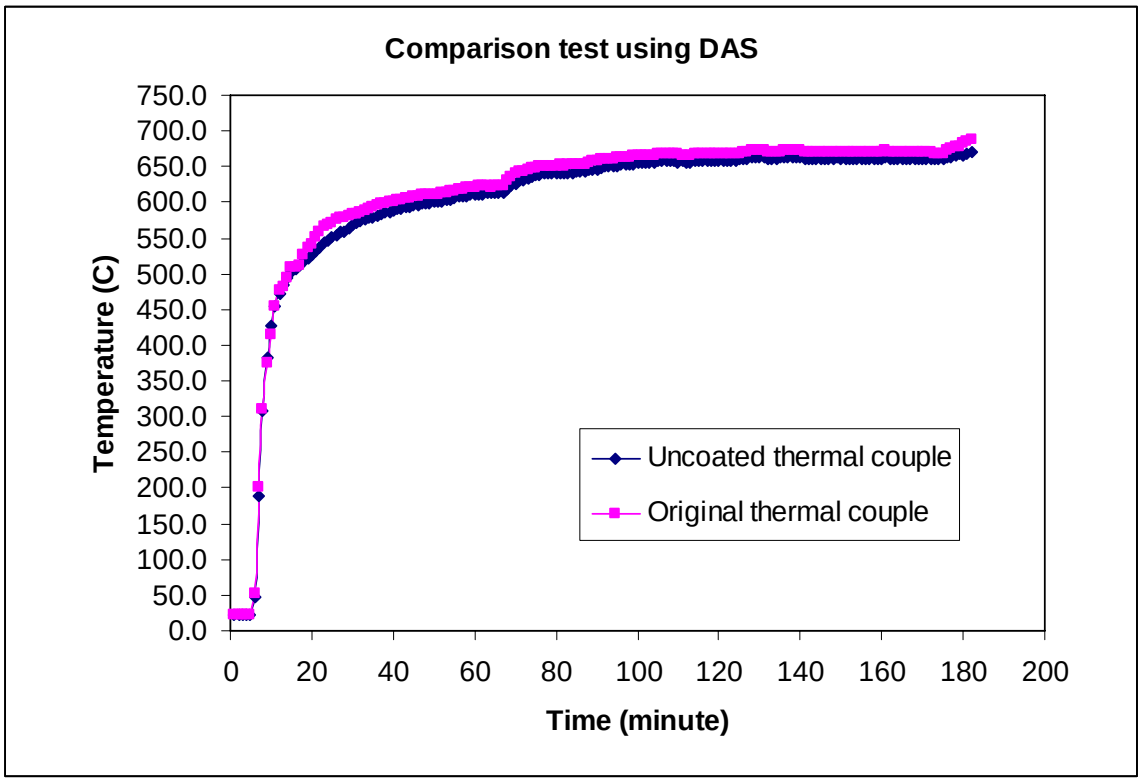

Figure 25 Comparison Tests of Coated/Uncoated Thermal Couple with DAS

Figures 26-29 show the comparison tests of coated and uncoated thermal couples under the conditions of 150 grams for fine dust particles and four full combinations of different levels of the air flow and ammonia/water. The experiment conditions are shown in Table A-1 in appendix II for the experimental observations of number 5 to 8. The temperature plots also show the identical of the temperature readings for coated and uncoated thermal couples throughout the tests. The temperature for uncoated thermal couple is uniformly higher than that of the coated thermal couple. The average temperature differences for these conditions are shown in Table A-2 in Appendix II.

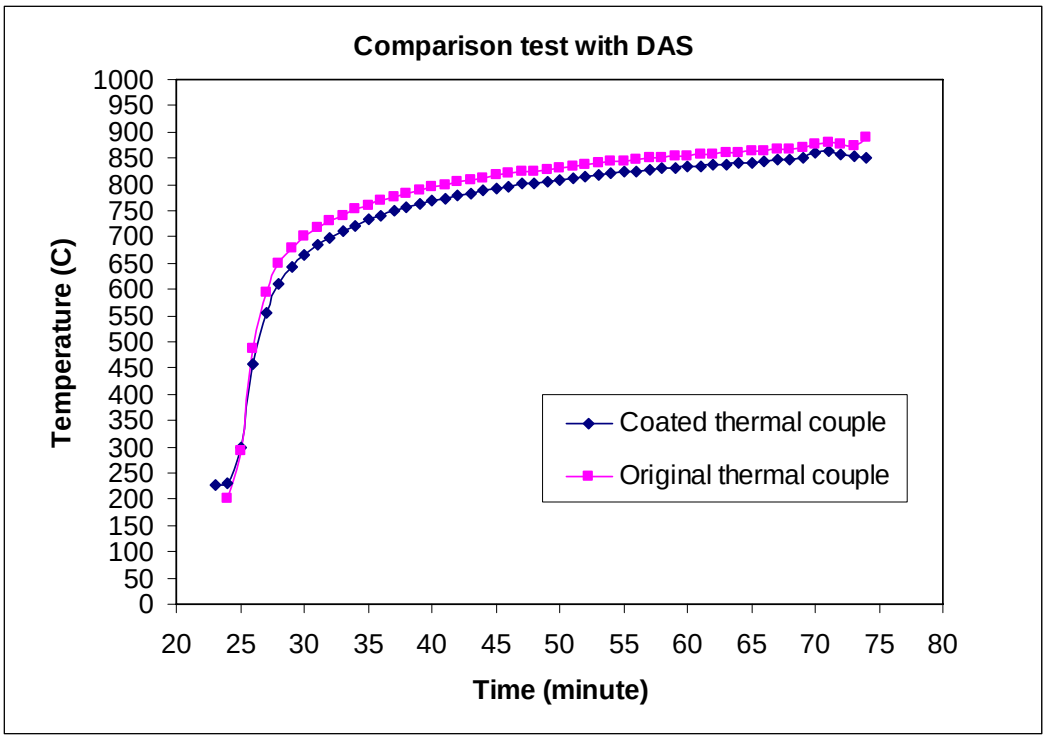

Figure 26 Comparison Tests of Coated/Uncoated Thermal Couple with DAS

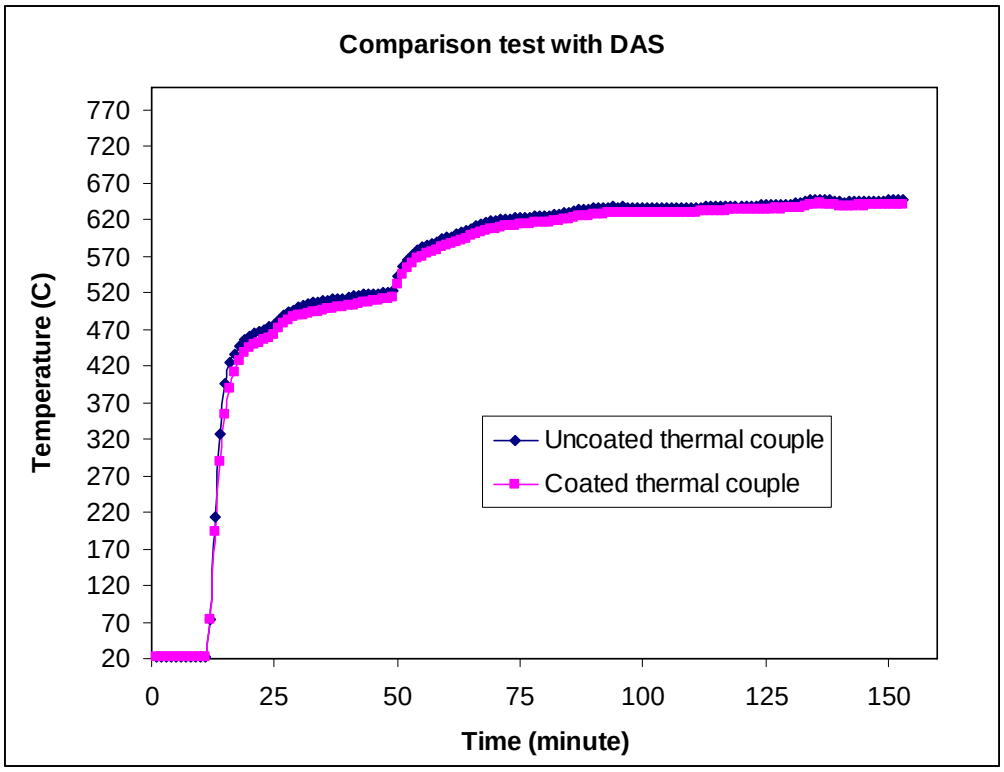

Figure 27 Comparison Tests of Coated/Uncoated Thermal Couple with DAS

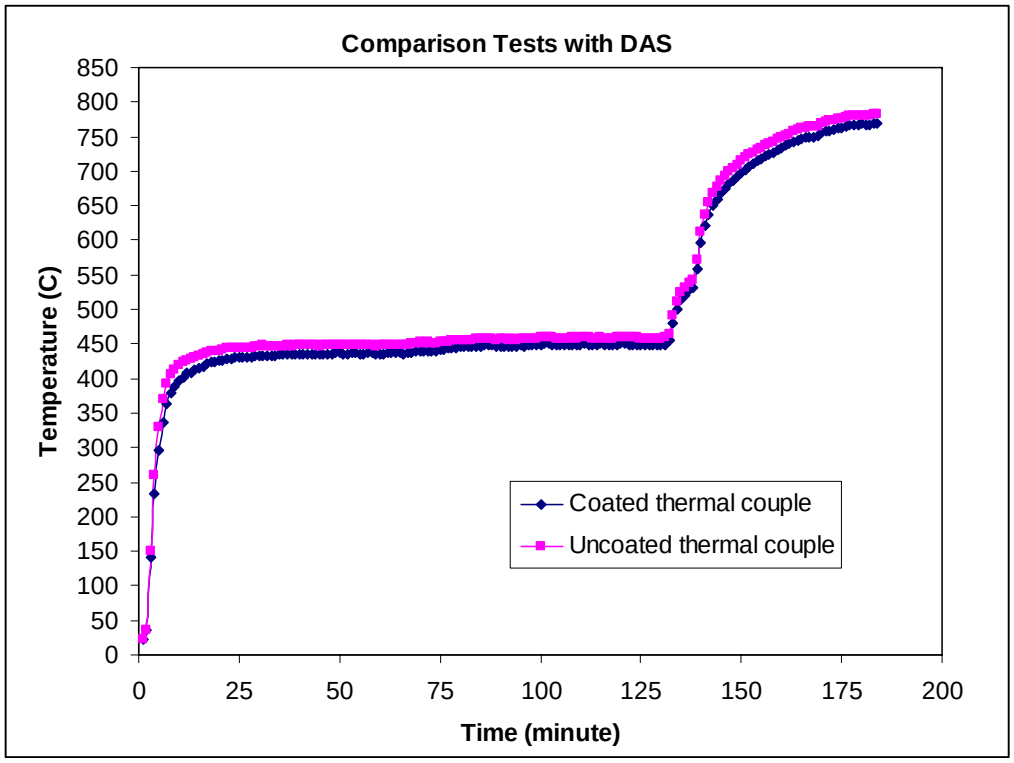

Figure 28 Comparison Tests of Coated/Uncoated Thermal Couple with DAS

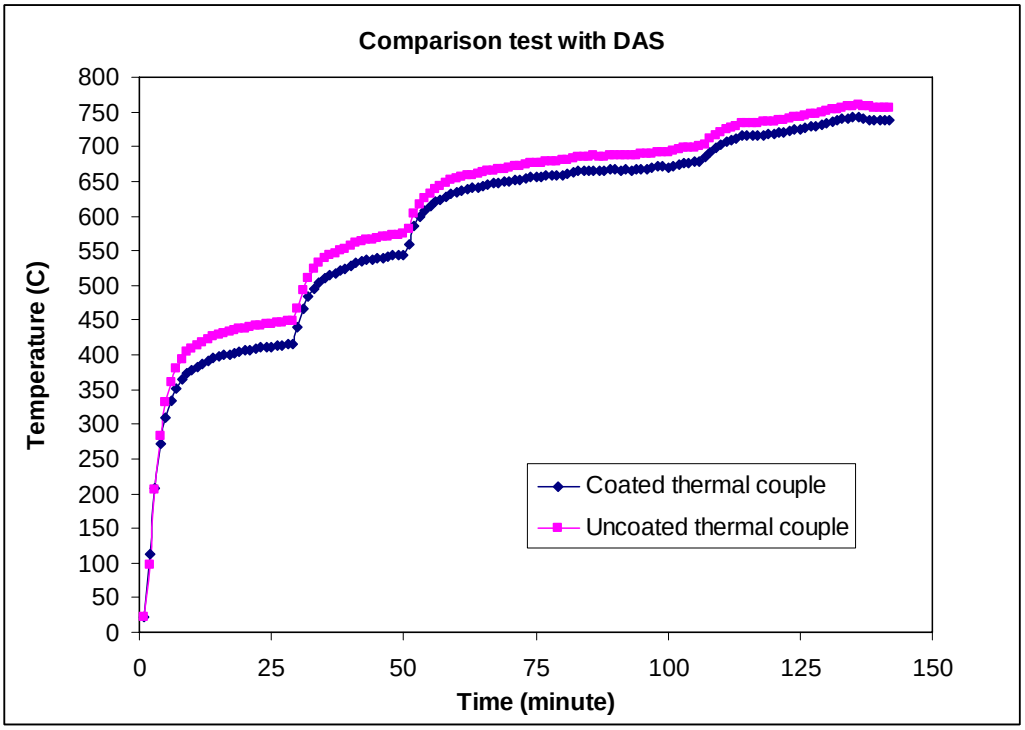

Figure 29 Comparison Tests of Coated/Uncoated Thermal Couple with DAS

5.4.2 Analysis of Variance (ANOVA)

ANOVA is used to uncover the main and interaction effects of the independent variables (called "factors") on an interval dependent variable (i.e. temperature difference)[31,32]. Table 5 shows the overall experiments results of the comparison of coated and uncoated thermal couples. Eight (8) experiments were conducted. The temperature difference between the coated and uncoated thermal couples is the real time average value of difference.

Table 5 Average Temperature Difference of Coated and Uncoated Thermal Couple

No. of experiments	Air flow	Ammonia/water flow	Fine dust particles amount	Averaged temperature difference
	Voltage	ml/minute	gram	C
1	15	2	75	8.7
2	10	2	75	15.4
3	15	3	75	9.4
4	10	3	75	23.2
5	15	2	150	10.4
6	10	2	150	9.0
7	15	3	150	12.9
8	10	3	150	22.0

In order to test whether the inside environments or operation conditions will affect the temperature measurement of the coated thermal couple, the temperature difference of two thermocouples were calculated. Furthermore, the temperature difference was computed with regard to different operational parameters such as airflow rate, water/ammonia flow rate and fine dust particles addition. The statistical software SPSS was used to compute the ANOVA Table as shown in Table 6. Table 6 includes column of parameter, sum of squared errors, degree of freedom (df), mean squared errors, F-test and significant level.

From the ANOVA Table, the factors of air flow rate, water/ammonia and fine dust are considered as non-significant factors at the type I error of α=0.05. This result indicates that the coated thermal couple does not affected by the operational parameters. Therefore, it is concluded that the coated thermal couple could be used to measure the temperate in the reducing and harsh environment.

Table 6 Analysis of Variance Table for the Comparison Tests

Parameters	Sum of Squares	Df	Mean Square	F	Sig.
Corrected Model	172.125(a)	3	57.375	3.437	.132
Intercept	1540.125	1	1540.125	92.264	.001
AirFlow	99.405	1	99.405	5.955	.071
WaterAmmonia	72.000	1	72.000	4.313	.106
FineDust	.720	1	.720	.043	.846
Error	66.770	4	16.693		
Total	1779.020	8			
Corrected Total	238.895	7			

a R Squared = .721 (Adjusted R Squared = .511)

6. Conclusions

The major conclusions are summarized as follows:

1. The cold and hot models of the gasification simulator have been successfully designed, fabricated and tested.
2. The electric motor of the irritating air blower affected the temperature behaviors in the cold model tests.
3. The techniques of design of experiment followed by the analysis of variances are very effective in experiment and data analysis.
4. The ultrasonic device was implemented for the feasibility study of the cleaning application in the gasifier
5. Linear and nonlinear regression methods are important tools to regress and predict the temperature distributions in the gasifier simulator (cold model and hot model); Nonlinear regression had a better performance in the prediction of the temperature changes in the gasifier
6. Water injection rate did not have the significant impact on the temperature measurements in the gasifier simulator, which proved the moisture immunity of the proposed temperature measurement device.
7. The air injection rate did have the significant impact on the temperature measurement in the gasifier simulator
8. The high-speed electric motor can be used to create the thermocouple vibration within the sub-sonic frequencies using unbalanced object at the motor shaft

9. The sub-sonic vibration could reduce the weight of the solid concrete cover layer on the thermocouple tip. The sub-sonic vibration frequency and amplitude are believed to have significant impacts on the concrete cover layer elimination process
10. The amount of fine dust particles has a significant effect on the temperature measurements. The temperature increases at steady state along with the increase of the amount of the fine dust particles.
11. The reducing environment in the gasifier simulator has a significant effect on the temperature readings. The temperature readings at steady state increase along the increase of the concentration of the ammonia hydroxide
12. The overall test matrix for hot model tests has been accomplished based on the central composite fractional factorial design. The significant factors for temperature readings are dust, water, air and ammonia. The un-balanced motor vibration is proved to be a non-significant factor.
13. Ultrasonic vibration is verified to have no significant effects on the temperature changes. These results may indicate that the ultrasonic vibration could be one of the best cleaning methods for thermocouple tip in the high temperature gasification environment
14. The effects of coated thermal couple of high velocity oxygen flow spray on the temperature measurement are uniformly distributed throughout the whole testing process under various test conditions
15. The temperature differences between the coated and uncoated thermal couples are not significant to the different combination of factors, which indicates that the coated thermal couples could be applied to the temperature measurement in the gasifier. The real temperature from the coated thermal couple could be calibrated by a constant.

16. The computerized data acquisition system (DAS) is designed and applied to the comparison test of the coated and uncoated thermal couples. The DAS is very useful and accurate for data recording and analysis.

References:

1. Coal Process Pollution Control, Thomas F. Edgar, Gulf Publish Company, 1983.
2. http://www.fe.doe.gov/coal_power/special_rpts/market_systems/market_sys.shtm.
3. http://www.netl.doe.gov/coalpower.
4. Duan Y., Investigation into coal gasification in an industrial jetting fluidized bed gasifier, Fuel and Energy Abstracts, Volume 43, Issue 4, July 2002, Page 249.
5. S.C. Bhattacharya, San Shwe Hla and Hoang-Luang Pham, A study on a multi-stage hybrid gasifier-engine system, Biomass and Bioenergy, Volume 21, Issue 6, December 2001, Pages 445-460.
6. Lee, S.W., "Effect of Solid-Bed Particles on the Material Wastage of In-Bed Tubes in the FBC", Presented at Fluids Engineering. Annual Conference & Exhibition, South Carolina, August 13-18, 1995, Book FED-Vol. 228, pp. 191-194.
7. Lee.S.W., and B.Q. Wang, " Erosion of AISI 1018 Steel and Several Thermal Sprayed Coatings under Simulated In-Bed Tube Erosion Conditions of Fluidized Bed Combustors", presented at 13th Int'L Conference FBC. Kissimmee, FL, May 7-10, 1995, Book FBC-Vol. 2, pp.1427-1432.
8. Lopamudra Devi, Krzysztof J. Ptasinski and Frans J.J. G. Janssen, A review of the primary measure for tar elimination in biomass gasification progress, Biomass and Bioenergy, Volume 24, Issue 2, February 2003, Pages 125-140.
9. Carlson C.P. Pian and Kunio Yoshikawa, Development of a high-temperature air-blown gasification system, Bioresource Technology, Volume 79, Issue 3, September 2001, Pages 231-241.
10. http://www.clarkson.edu/~microlab/Ultrason.htm.
11. Yourong Liu, Traugott E. Fischer and Andrew Dent, Comparison of HVOF and plasma-sprayed alumina/titania coatings-microstructure, mechanical properties and abrasion behavior, Surface and Coatings Technology, Volume 167, Issue 1, 1 April 2003, Pages 68-76.
12. Montgomery D. C. , Design and Analysis of experiments, 4th Edition, 1997.
13. Anderson, Mark J., Patrick J. Whitcomb, An Introduction to Design of Experiments: A Simplified Approach, American Society for Quality; ISBN: 0873894448, January 1999.
14. Abramov, O.V., High-Intensity Ultrasonics: Theory and Industrial Applications, CRC Press, ISBN: 9056990411, November 1, 1998
15. Papadakis, E. P., Ultrasonic Instruments and Devices, Academic Press, ISBN: 0125319517, January 2000.
16. Lee, S. W., "Innovative Instrumentation and Analysis of the Temperature Measurement for High Tmeperature Gasification" DOE Progress Report II, October 2003.
17. Gexue, R., L. Qiuhai, H. Ning, N. Rendong, and N. Bo, On Vibration Control with Steward Parallel Mechanism, Mechatronics, Feb 2004.
18. Antoni, J. and R.B. Randall, Unsupervised Noise Cancellation for Vibration Signals: Part I-Evaluation of Adaptive Algorithms, Mechanical Systems and Signal Processing, Jan 2004
19. Tsujino, J. K. Hidai, A. Hasegawa, R. Kanai, H. Matsuura, K. Matsushima, T. Ueoka, Ultrasonic Butt Welding of Aluminum, Aluminum Alloy and Stainless Steel Plate Specimens, Ultrasonic , May 2002.
20. Ku, H.S., F. Siu, E. Siores, J.A.R. Ball, Variable Frequency Microware(VFM) Processing Facilities and Application in Processing Thermoplastic Matrix Composites, Journal of Adhesion and Adhesives, Jan 2003.

21. Chrome Plating Alternative Thermal Spray: http://www.faculty.rsu.edu/~clayton/kalivas/paper.htm
22. http://www.fe.doe.gov/coal_power/special-rpts/market_systems/market_sys.shtm
23. High Velocity Oxygen Fuel Thermal Spray Process: http://www.gordonengland..co.uk/hvof.htm
24. R. Ghafouri-Azar, J. Mostaghimi and S. Chandra, Modeling development of residual stresses in thermal spray coatings, Computational Materials Science, Volume 35, Issue 1, January 2006, Pages 13-26
25. J. Vicenzi, D.L. Villanova, M.D. Lima, A.S. Takimi, C.M. Marques and C.P. Bergmann, HVOF-coatings against high temperature erosion(~300 ^0C) by coal fly ash in thermoelectric power plant, Materials & Design, Volume 27, Issue 3, 2006, Pages 236-242
26. Josep A. Picas, Antonio Form, Ramiro Rilla and Enric Martin, HVOF thermal sprayed coatings on aluminium alloys and aluminium matrix composites Surface and Coatings Technology, Vol. 200, Issue 1-4, 1 October 2005, Pages 1178-1181
27. Lee, S.W., Semi-Annual Report: "Innovative Instrumentation and Analysis of the Temperature Measurement for High Temperature Gasification", DOE report, April 04
28. Sonbond Ultrasonics Company, Operating Manual of Hand Welding Device Hg 20-1, 2003.
29. R.H. Myers, D.C. Montgomery, Response Surface Methodology: Process and Product Optimization using Designed Experiments, 2nd edition, John Willey and Sons, Inc., 2004
30. User's Guide, OMB-DAQ-54/55/56 quick start guide. Omega, 2005
31. Zhu, S., Y. Liu, J. Ngeru and S.W. Lee, "Innovative High Temperature Measurement and Analysis in a Gasifier Simulator", presented and published in the Proceedings of 11th Annual Undergraduate and Graduate Science Research Symposium , April 2004, Baltimore MD.
32. D.C. Montgomery, Design and Analysis of Experiments, 6th edition, John Willey and Sons, Inc., 2004

Appendix 1:

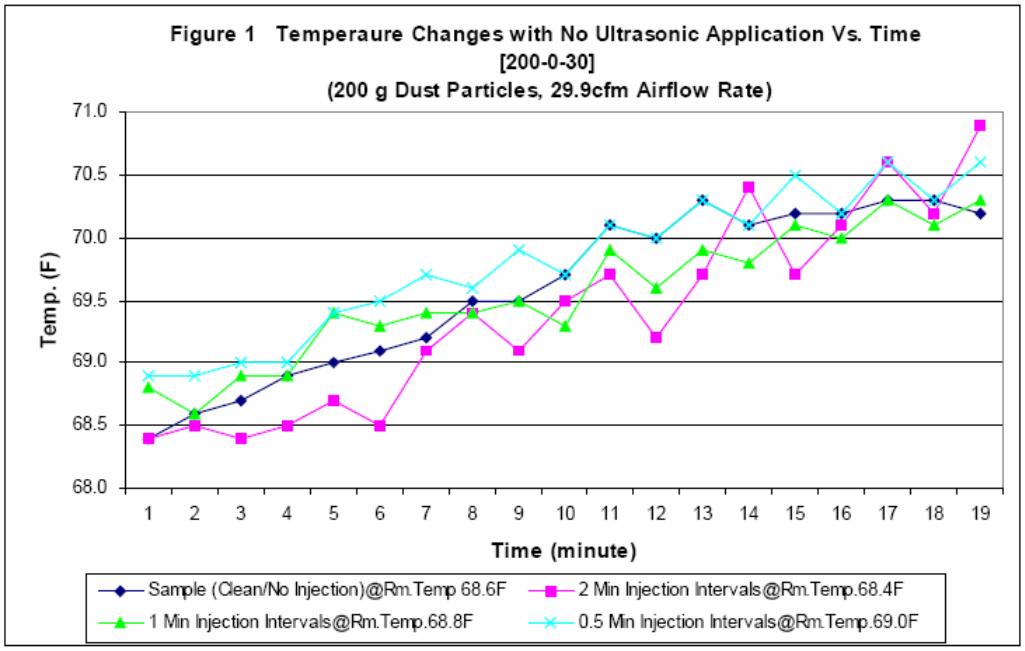
Figure 1 Temperaure Changes with No Ultrasonic Application Vs. Time
[200-0-30]
(200 g Dust Particles, 29.9cfm Airflow Rate)
Temp. (F)
71.0
70.5
70.0
69.5
69.0
68.5
68.0
1 2 3 4 5 6 7 8 9 10 11 12 13 14 15 16 17 18 19
Time (minute)
Sample (Clean/No Injection)@Rm.Temp 68.6F
2 Min Injection Intervals@Rm.Temp.68.4F
1 Min Injection Intervals@Rm.Temp.68.8F
0.5 Min Injection Intervals@Rm.Temp.69.0F

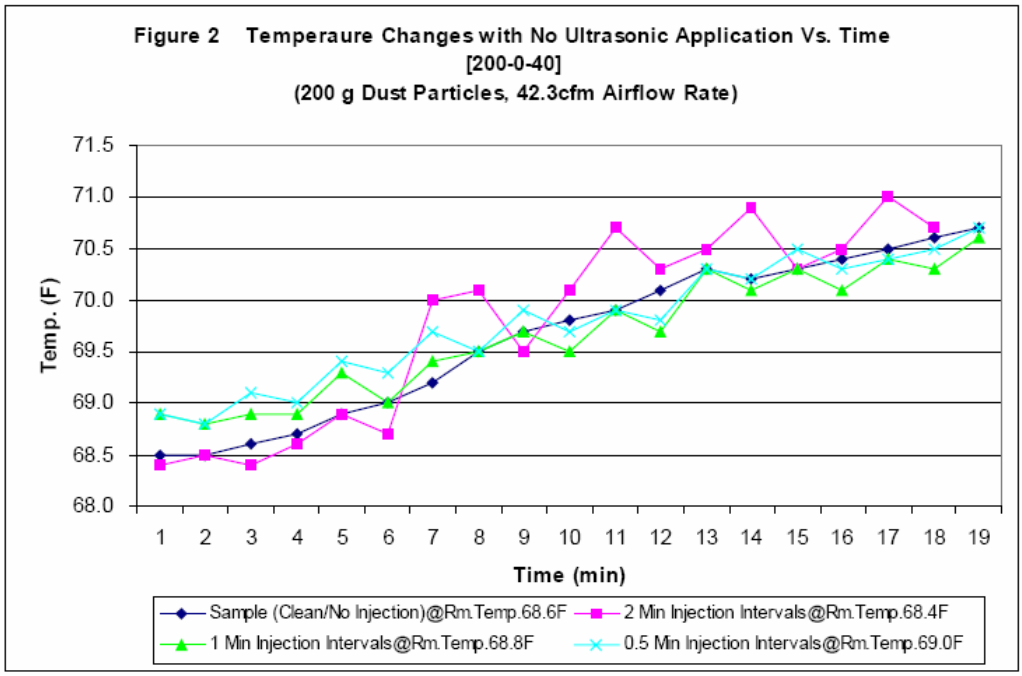
Figure 2 Temperaure Changes with No Ultrasonic Application Vs. Time
[200-0-40]
(200 g Dust Particles, 42.3cfm Airflow Rate)
Temp. (F)
71.5
71.0
70.5
70.0
69.5
69.0
68.5
68.0
1 2 3 4 5 6 7 8 9 10 11 12 13 14 15 16 17 18 19
Time (min)
Sample (Clean/No Injection)@Rm.Temp.68.6F
2 Min Injection Intervals@Rm.Temp.68.4F
1 Min Injection Intervals@Rm.Temp.68.8F
0.5 Min Injection Intervals@Rm.Temp.69.0F

Figure 3 Temperaure Changes with No Ultrasonic Application Vs. Time
[200-0-50]
(200 g Dust Particles, 53.5cfm Airflow Rate)

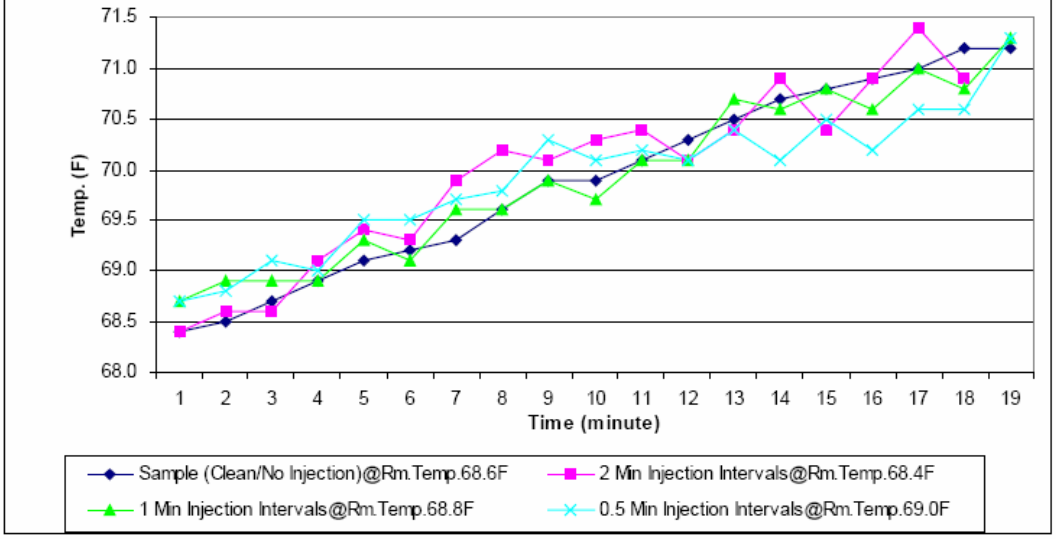

Figure 4 Temperature Changes with 1 Ultrasonic Application Vs. Time
[200-1-30]
(200 g Dust Particles, 29.9cfm Airflow Rate)

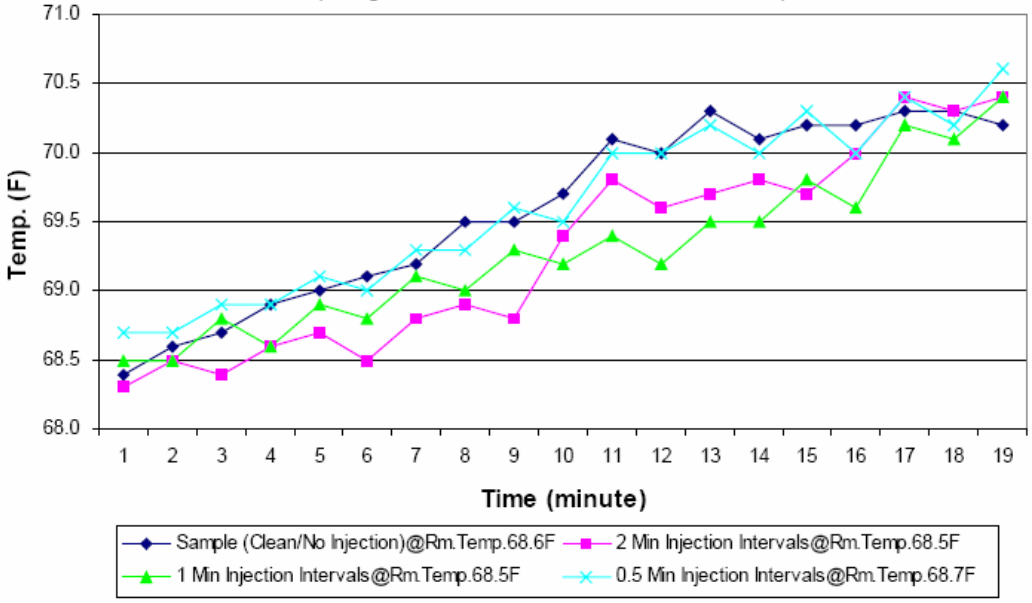

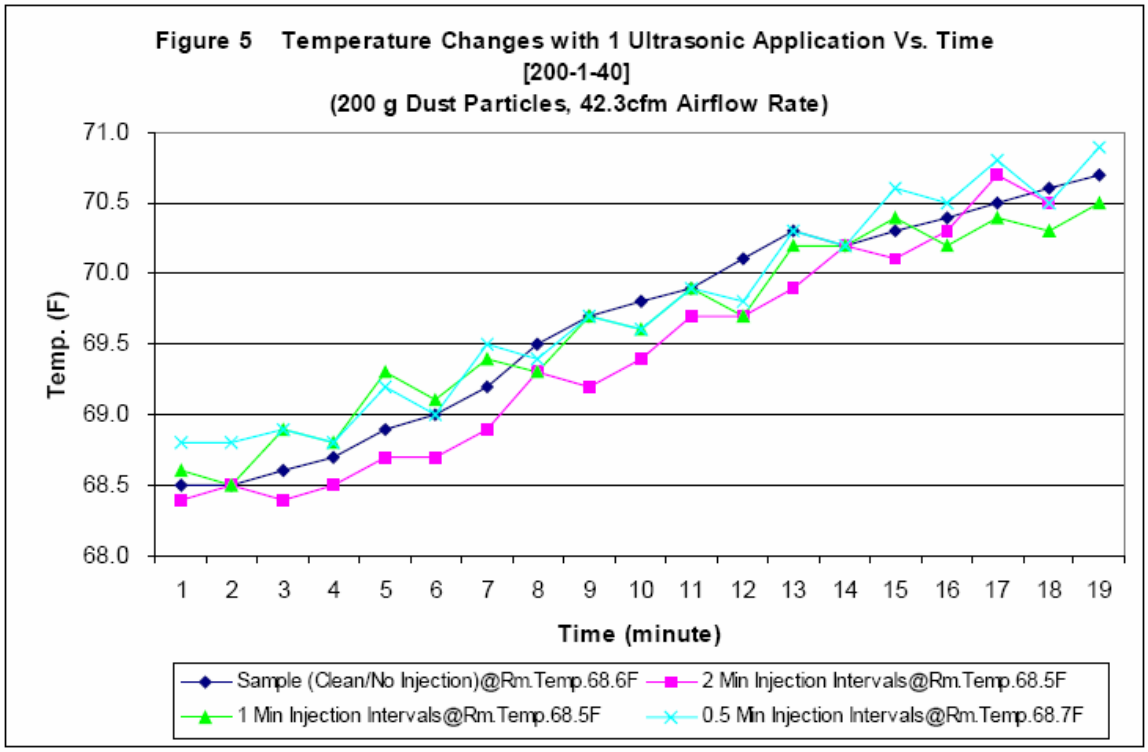
Figure 5 Temperature Changes with 1 Ultrasonic Application Vs. Time
[200-1-40]
(200 g Dust Particles, 42.3cfm Airflow Rate)
Temp. (F)
71.0
70.5
70.0
69.5
69.0
68.5
68.0
1 2 3 4 5 6 7 8 9 10 11 12 13 14 15 16 17 18 19
Time (minute)
Sample (Clean/No Injection)@Rm.Temp.68.6F
2 Min Injection Intervals@Rm.Temp.68.5F
1 Min Injection Intervals@Rm.Temp.68.5F
0.5 Min Injection Intervals@Rm.Temp.68.7F

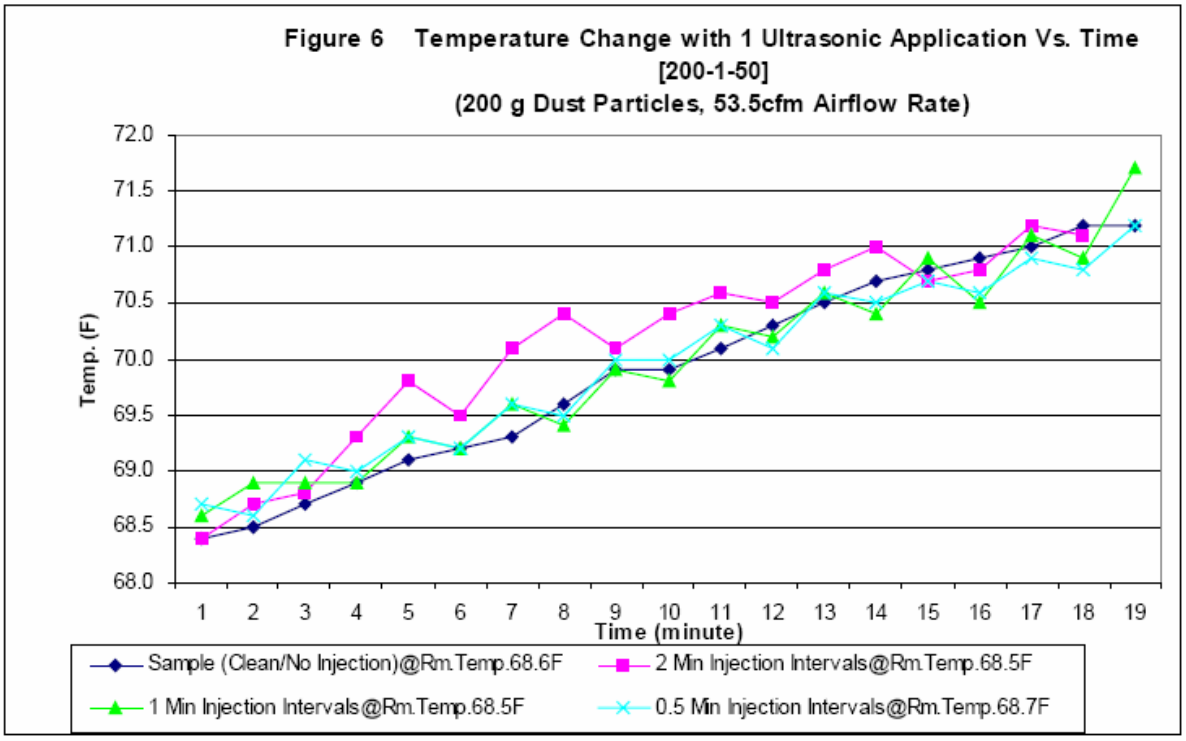
Figure 6 Temperature Change with 1 Ultrasonic Application Vs. Time
[200-1-50]
(200 g Dust Particles, 53.5cfm Airflow Rate)
Temp. (F)
72.0
71.5
71.0
70.5
70.0
69.5
69.0
68.5
68.0
1 2 3 4 5 6 7 8 9 10 11 12 13 14 15 16 17 18 19
Time (minute)
Sample (Clean/No Injection)@Rm.Temp.68.6F
2 Min Injection Intervals@Rm.Temp.68.5F
1 Min Injection Intervals@Rm.Temp.68.5F
0.5 Min Injection Intervals@Rm.Temp.68.7F

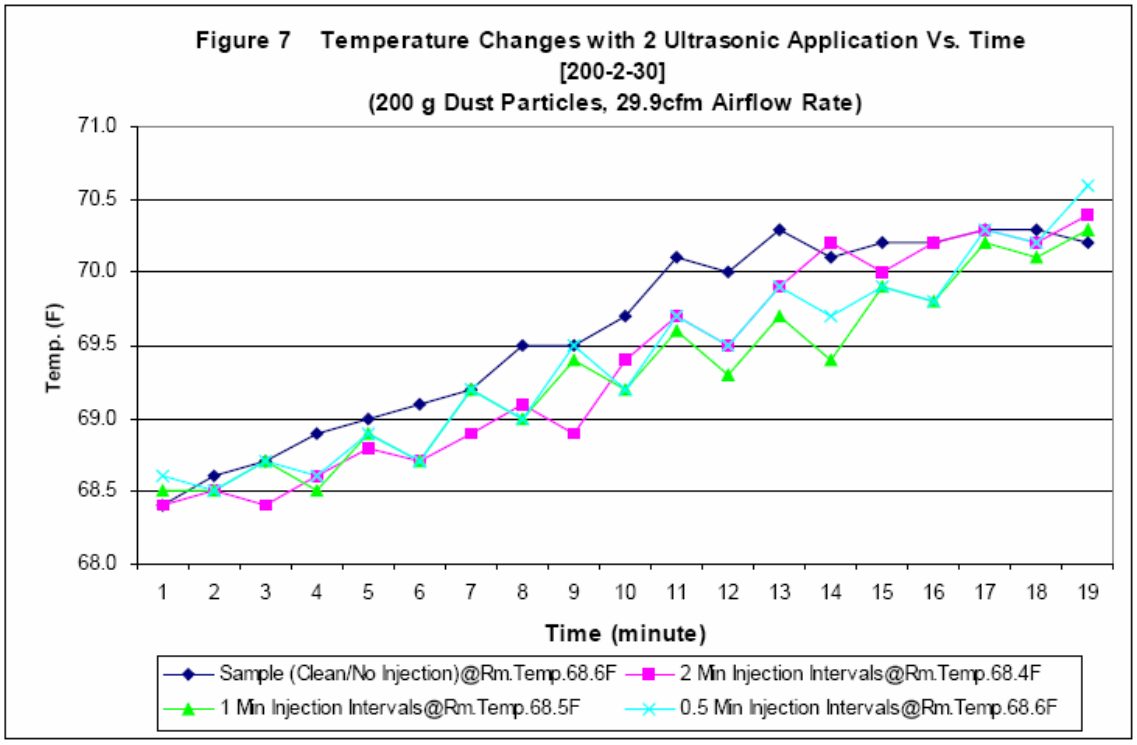
Figure 7 Temperature Changes with 2 Ultrasonic Application Vs. Time
[200-2-30]
(200 g Dust Particles, 29.9cfm Airflow Rate)
71.0
70.5
70.0
69.5
69.0
68.5
68.0
Temp. (F)
1 2 3 4 5 6 7 8 9 10 11 12 13 14 15 16 17 18 19
Time (minute)
Sample (Clean/No Injection)@Rm.Temp.68.6F
2 Min Injection Intervals@Rm.Temp.68.4F
1 Min Injection Intervals@Rm.Temp.68.5F
0.5 Min Injection Intervals@Rm.Temp.68.6F

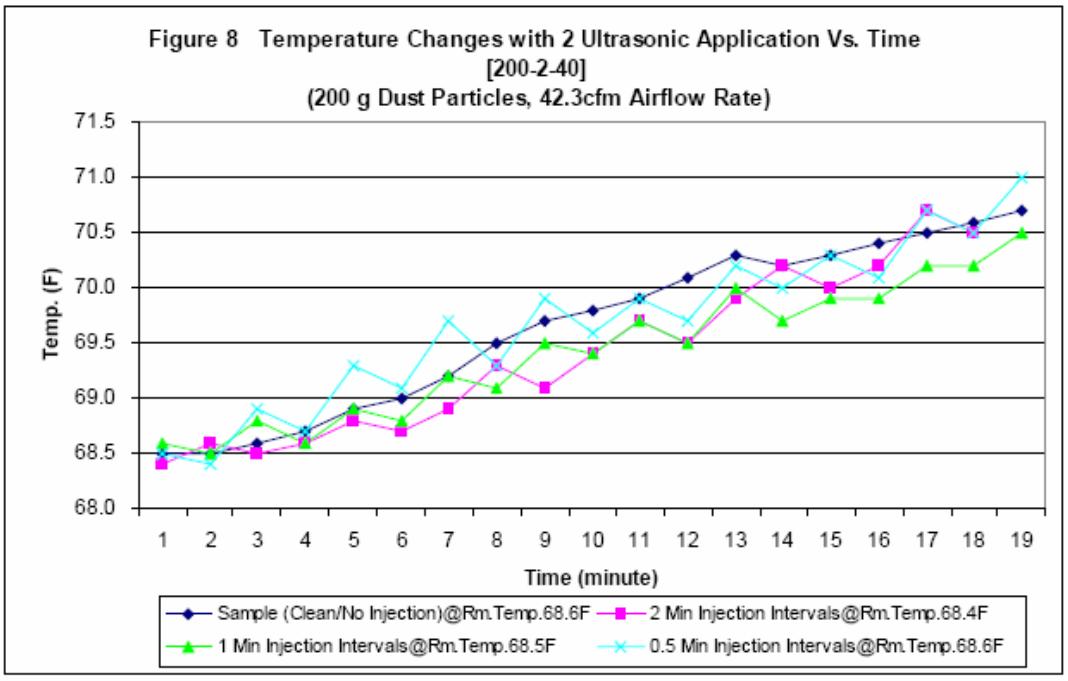
Figure 8 Temperature Changes with 2 Ultrasonic Application Vs. Time
[200-2-40]
(200 g Dust Particles, 42.3cfm Airflow Rate)
71.5
71.0
70.5
70.0
69.5
69.0
68.5
68.0
Temp. (F)
1 2 3 4 5 6 7 8 9 10 11 12 13 14 15 16 17 18 19
Time (minute)
Sample (Clean/No Injection)@Rm.Temp.68.6F
2 Min Injection Intervals@Rm.Temp.68.4F
1 Min Injection Intervals@Rm.Temp.68.5F
0.5 Min Injection Intervals@Rm.Temp.68.6F

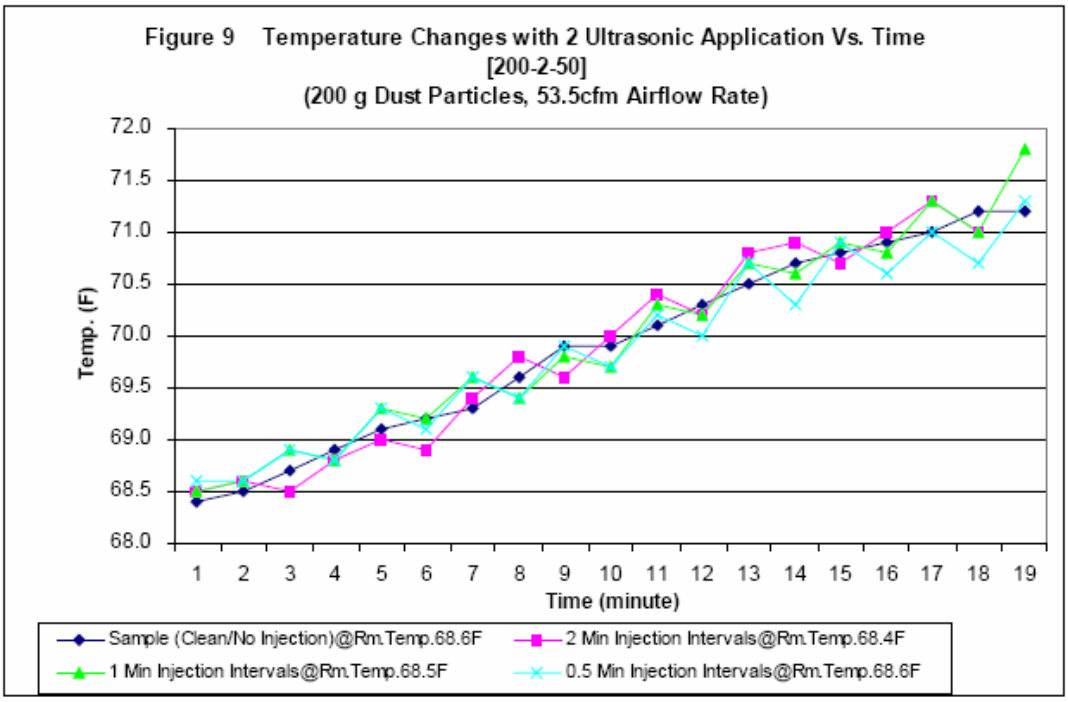
Figure 9 Temperature Changes with 2 Ultrasonic Application Vs. Time
[200-2-50]
(200 g Dust Particles, 53.5cfm Airflow Rate)
Temp. (F)
72.0
71.5
71.0
70.5
70.0
69.5
69.0
68.5
68.0
1 2 3 4 5 6 7 8 9 10 11 12 13 14 15 16 17 18 19
Time (minute)
Sample (Clean/No Injection)@Rm.Temp.68.6F
2 Min Injection Intervals@Rm.Temp.68.4F
1 Min Injection Intervals@Rm.Temp.68.5F
0.5 Min Injection Intervals@Rm.Temp.68.6F

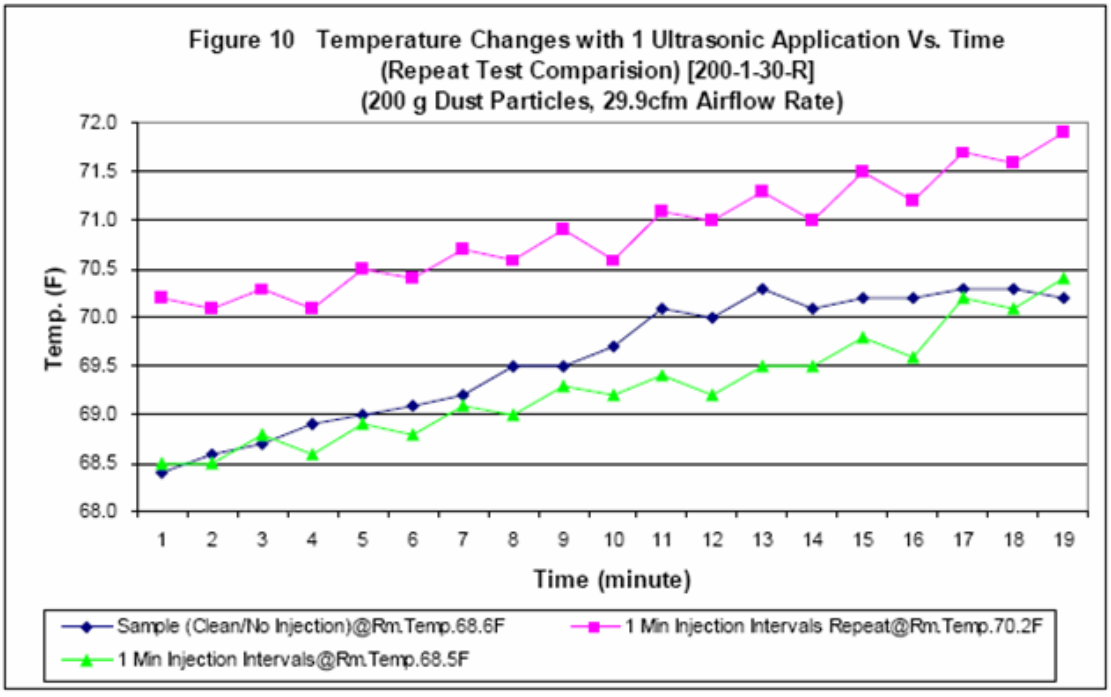
Figure 10 Temperature Changes with 1 Ultrasonic Application Vs. Time
(Repeat Test Comparision) [200-1-30-R]
(200 g Dust Particles, 29.9cfm Airflow Rate)
Temp. (F)
72.0
71.5
71.0
70.5
70.0
69.5
69.0
68.5
68.0
1 2 3 4 5 6 7 8 9 10 11 12 13 14 15 16 17 18 19
Time (minute)
Sample (Clean/No Injection)@Rm.Temp.68.6F
1 Min Injection Intervals Repeat@Rm.Temp.70.2F
1 Min Injection Intervals@Rm.Temp.68.5F

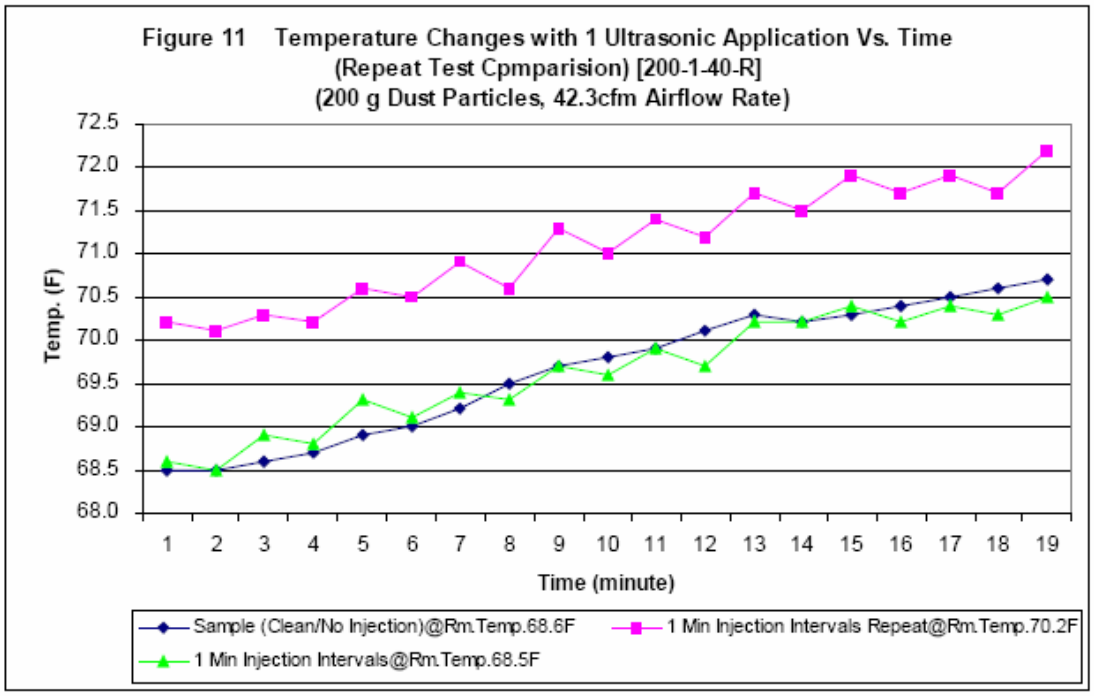
Figure 11 Temperature Changes with 1 Ultrasonic Application Vs. Time
(Repeat Test Cpmparision) [200-1-40-R]
(200 g Dust Particles, 42.3cfm Airflow Rate)
Temp. (F)
72.5
72.0
71.5
71.0
70.5
70.0
69.5
69.0
68.5
68.0
1 2 3 4 5 6 7 8 9 10 11 12 13 14 15 16 17 18 19
Time (minute)
Sample (Clean/No Injection)@Rm.Temp.68.6F
1 Min Injection Intervals Repeat@Rm.Temp.70.2F
1 Min Injection Intervals@Rm.Temp.68.5F

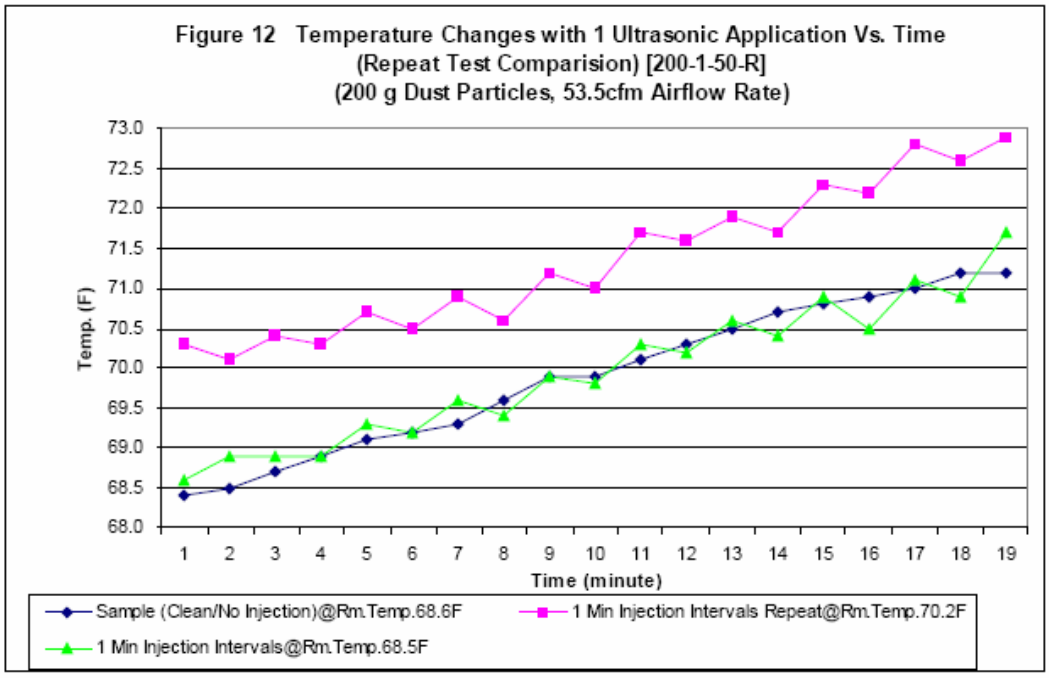
Figure 12 Temperature Changes with 1 Ultrasonic Application Vs. Time
(Repeat Test Comparision) [200-1-50-R]
(200 g Dust Particles, 53.5cfm Airflow Rate)
Temp. (F)
73.0
72.5
72.0
71.5
71.0
70.5
70.0
69.5
69.0
68.5
68.0
1 2 3 4 5 6 7 8 9 10 11 12 13 14 15 16 17 18 19
Time (minute)
Sample (Clean/No Injection)@Rm.Temp.68.6F
1 Min Injection Intervals Repeat@Rm.Temp.70.2F
1 Min Injection Intervals@Rm.Temp.68.5F

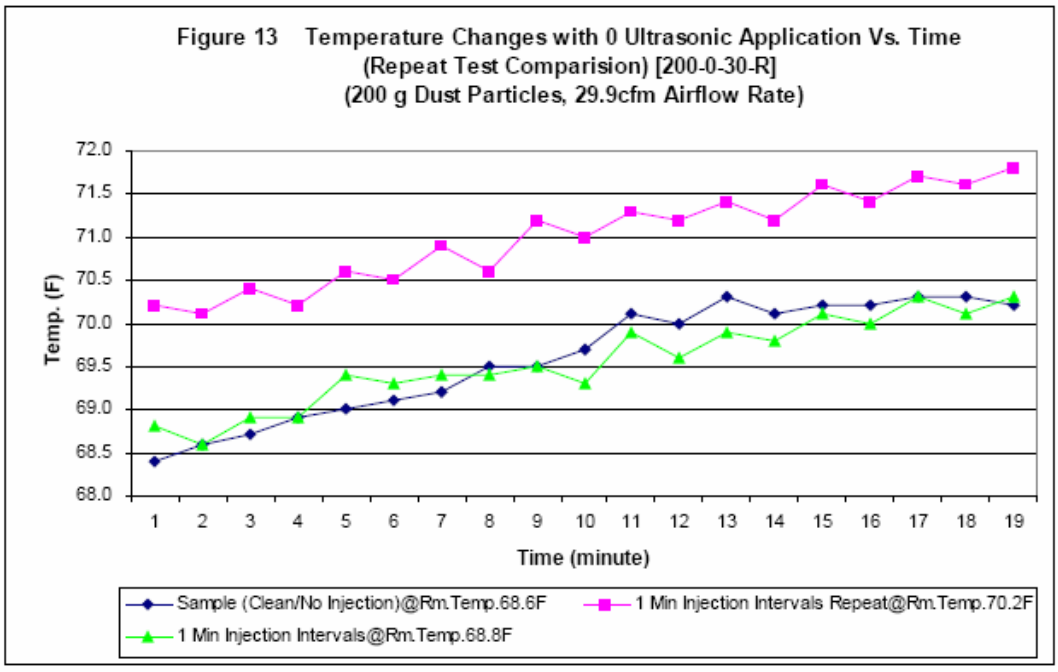
Figure 13 Temperature Changes with 0 Ultrasonic Application Vs. Time
(Repeat Test Comparision) [200-0-30-R]
(200 g Dust Particles, 29.9cfm Airflow Rate)
Temp. (F)
72.0
71.5
71.0
70.5
70.0
69.5
69.0
68.5
68.0
1 2 3 4 5 6 7 8 9 10 11 12 13 14 15 16 17 18 19
Time (minute)
Sample (Clean/No Injection)@Rm.Temp.68.6F
1 Min Injection Intervals Repeat@Rm.Temp.70.2F
1 Min Injection Intervals@Rm.Temp.68.8F

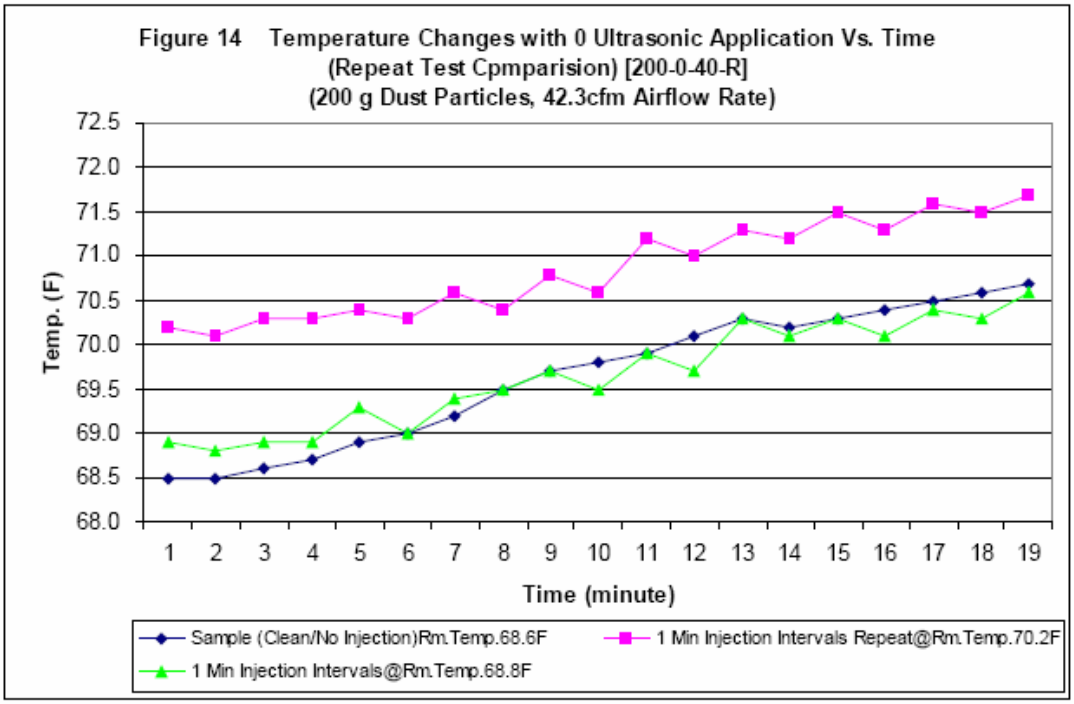
Figure 14 Temperature Changes with 0 Ultrasonic Application Vs. Time
(Repeat Test Cpmparision) [200-0-40-R]
(200 g Dust Particles, 42.3cfm Airflow Rate)
Temp. (F)
72.5
72.0
71.5
71.0
70.5
70.0
69.5
69.0
68.5
68.0
1 2 3 4 5 6 7 8 9 10 11 12 13 14 15 16 17 18 19
Time (minute)
Sample (Clean/No Injection)Rm.Temp.68.6F
1 Min Injection Intervals Repeat@Rm.Temp.70.2F
1 Min Injection Intervals@Rm.Temp.68.8F

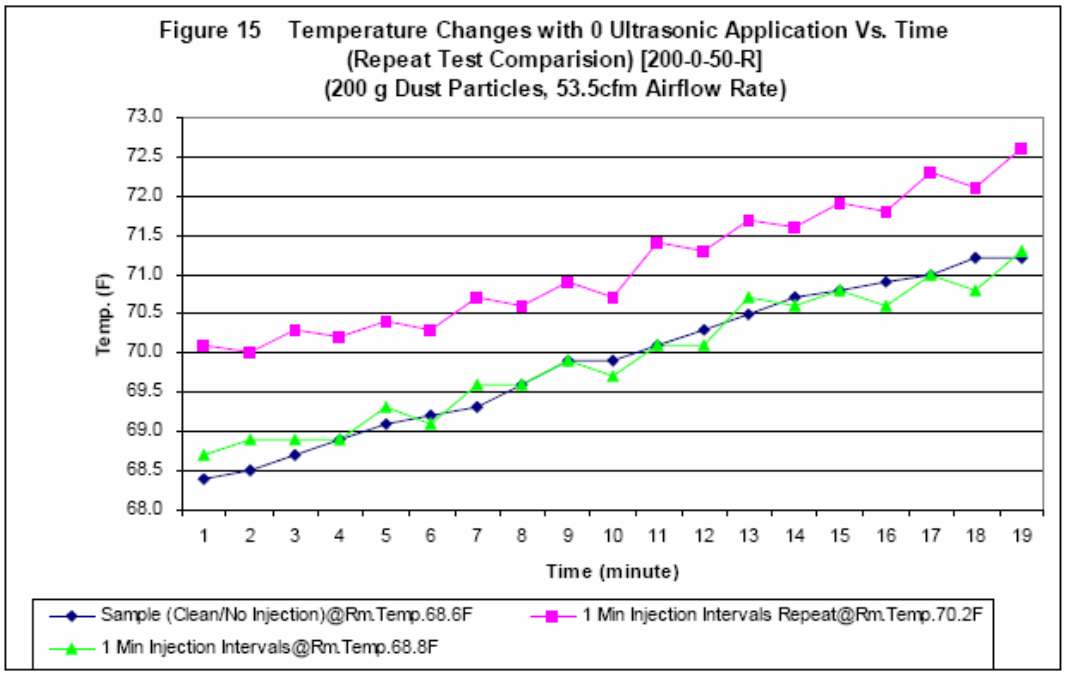
Figure 15 Temperature Changes with 0 Ultrasonic Application Vs. Time
(Repeat Test Comparision) [200-0-50-R]
(200 g Dust Particles, 53.5cfm Airflow Rate)
Temp. (F)
Time (minute)
Sample (Clean/No Injection)@Rm.Temp.68.6F
1 Min Injection Intervals Repeat@Rm.Temp.70.2F
1 Min Injection Intervals@Rm.Temp.68.8F

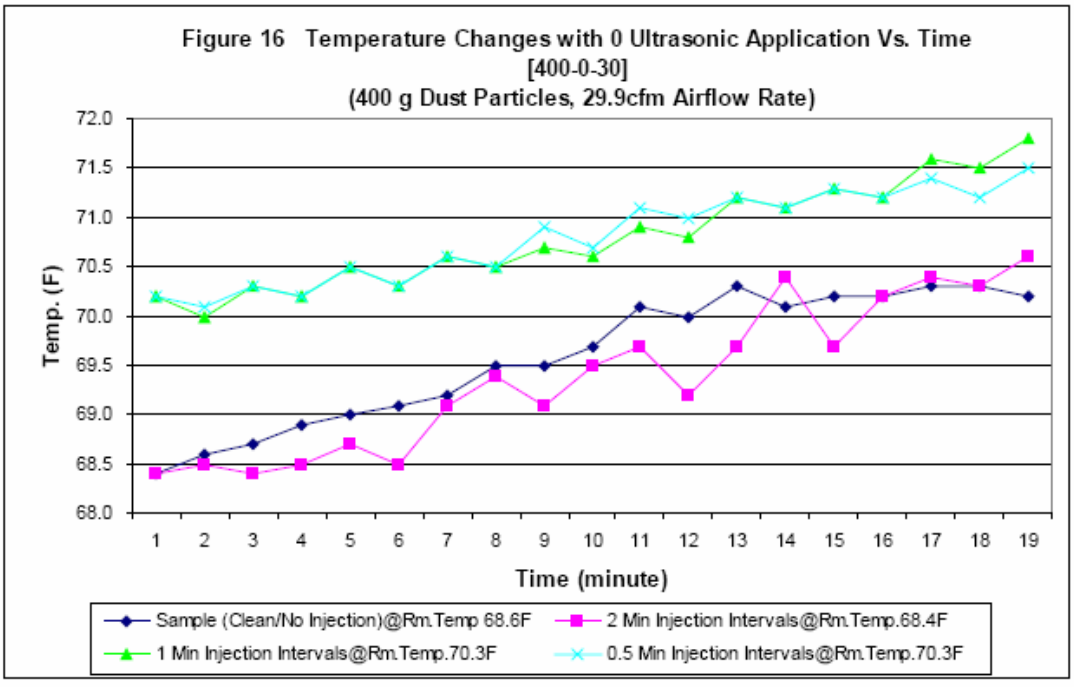
Figure 16 Temperature Changes with 0 Ultrasonic Application Vs. Time
[400-0-30]
(400 g Dust Particles, 29.9cfm Airflow Rate)
Temp. (F)
Time (minute)
Sample (Clean/No Injection)@Rm.Temp 68.6F
2 Min Injection Intervals@Rm.Temp.68.4F
1 Min Injection Intervals@Rm.Temp.70.3F
0.5 Min Injection Intervals@Rm.Temp.70.3F

Figure 17 Temperature Changes with 0 Ultrasonic Application Vs. Time
[400-0-40]
(400 g Dust Particles, 42.3cfm Airflow Rate)

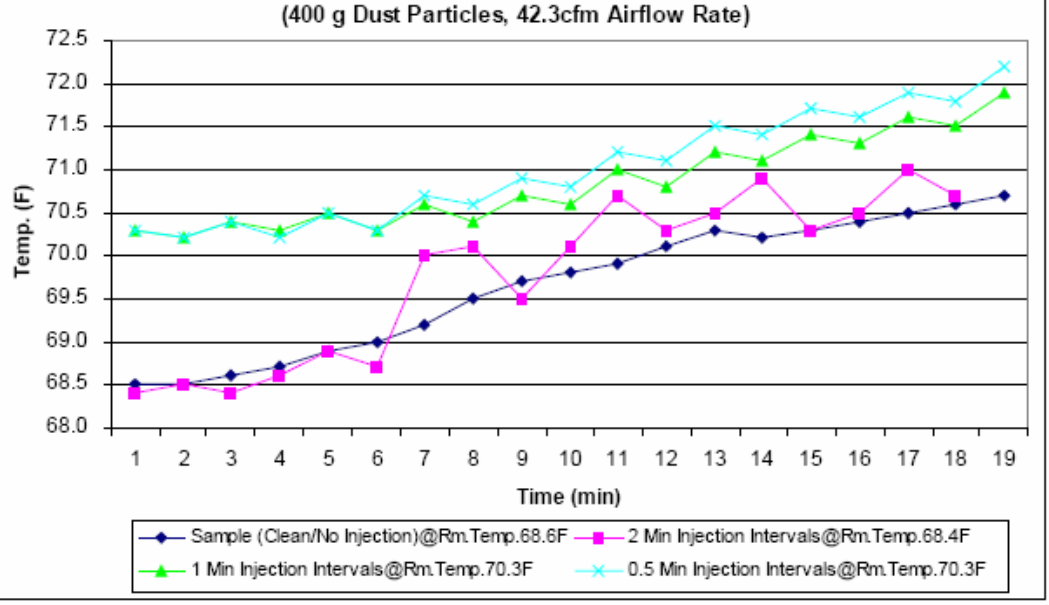

Figure 18 Temperature Changes with 0 Ultrasonic Application Vs. Time
[400-0-50]
(400 g Dust Particles, 53.5cfm Airflow Rate)

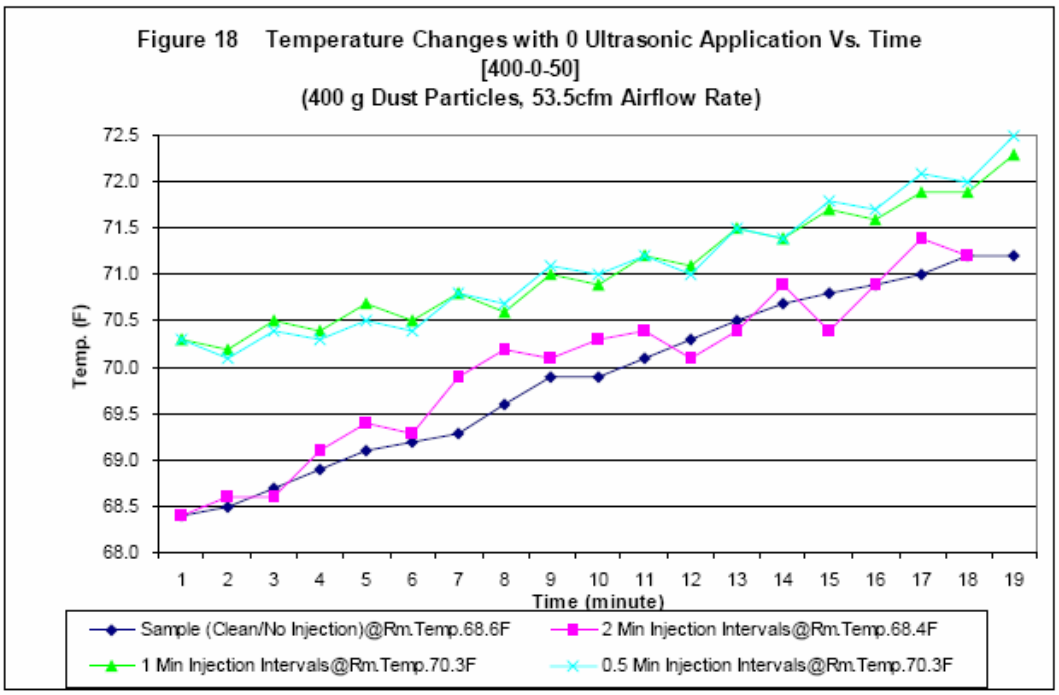

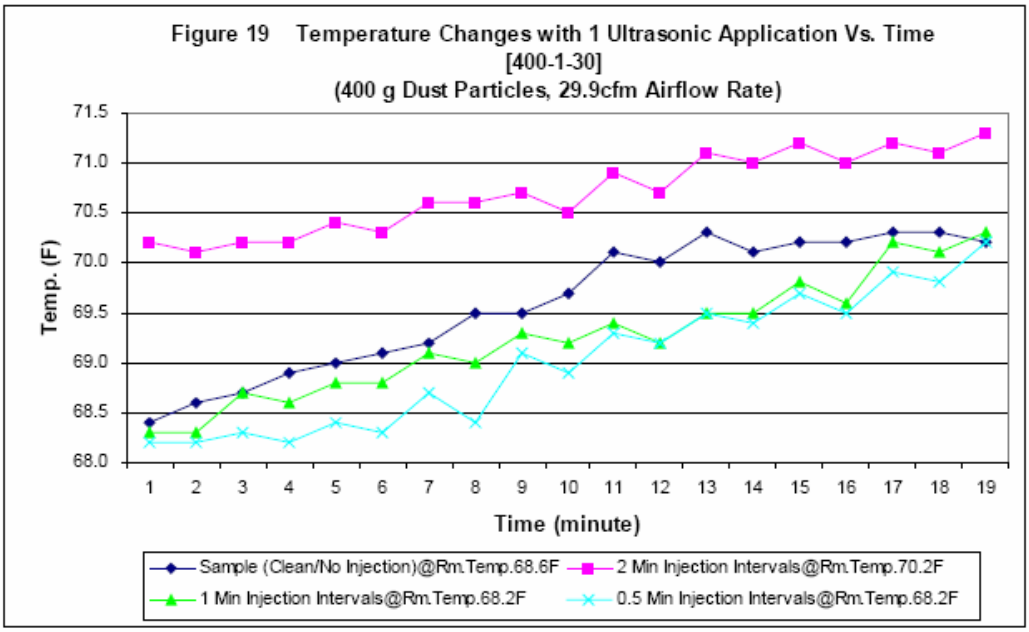
Figure 19 Temperature Changes with 1 Ultrasonic Application Vs. Time
[400-1-30]
(400 g Dust Particles, 29.9cfm Airflow Rate)
Temp. (F)
71.5
71.0
70.5
70.0
69.5
69.0
68.5
68.0
1 2 3 4 5 6 7 8 9 10 11 12 13 14 15 16 17 18 19
Time (minute)
Sample (Clean/No Injection)@Rm.Temp.68.6F
2 Min Injection Intervals@Rm.Temp.70.2F
1 Min Injection Intervals@Rm.Temp.68.2F
0.5 Min Injection Intervals@Rm.Temp.68.2F

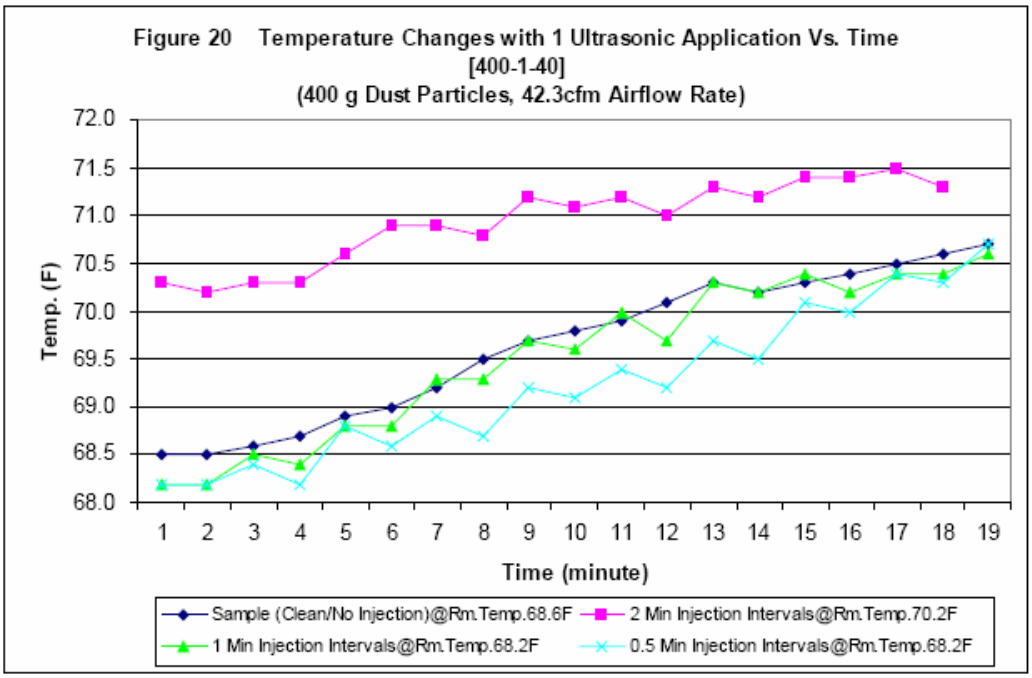
Figure 20 Temperature Changes with 1 Ultrasonic Application Vs. Time
[400-1-40]
(400 g Dust Particles, 42.3cfm Airflow Rate)
Temp. (F)
72.0
71.5
71.0
70.5
70.0
69.5
69.0
68.5
68.0
1 2 3 4 5 6 7 8 9 10 11 12 13 14 15 16 17 18 19
Time (minute)
Sample (Clean/No Injection)@Rm.Temp.68.6F
2 Min Injection Intervals@Rm.Temp.70.2F
1 Min Injection Intervals@Rm.Temp.68.2F
0.5 Min Injection Intervals@Rm.Temp.68.2F

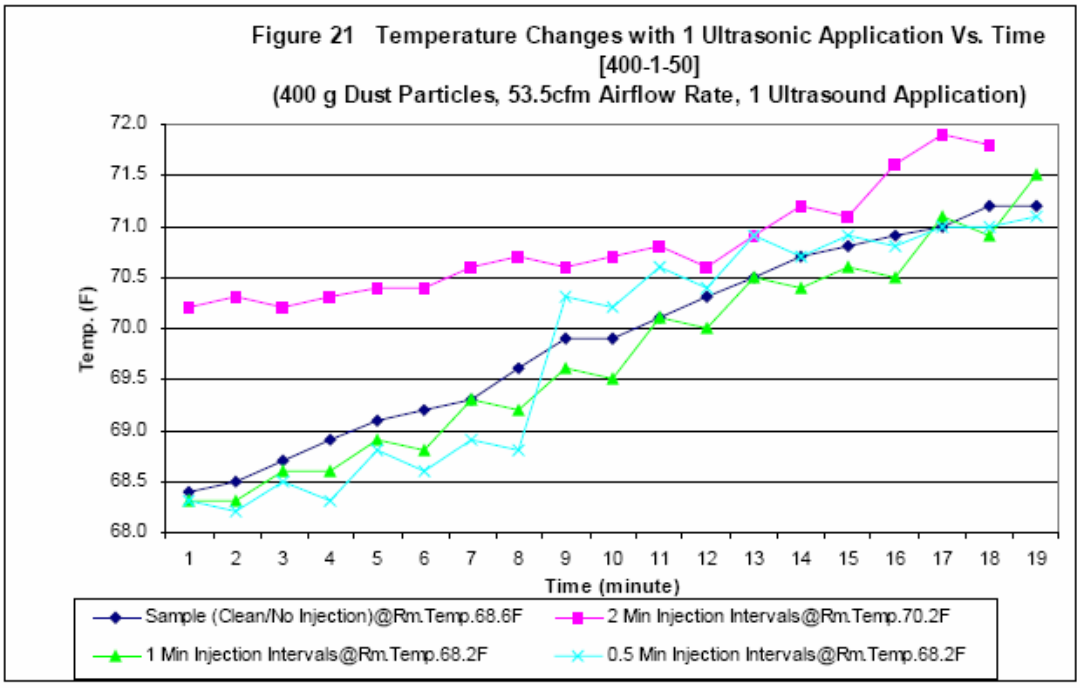
Figure 21 Temperature Changes with 1 Ultrasonic Application Vs. Time
[400-1-50]
(400 g Dust Particles, 53.5cfm Airflow Rate, 1 Ultrasound Application)
Temp. (F)
72.0
71.5
71.0
70.5
70.0
69.5
69.0
68.5
68.0
1 2 3 4 5 6 7 8 9 10 11 12 13 14 15 16 17 18 19
Time (minute)
Sample (Clean/No Injection)@Rm.Temp.68.6F
2 Min Injection Intervals@Rm.Temp.70.2F
1 Min Injection Intervals@Rm.Temp.68.2F
0.5 Min Injection Intervals@Rm.Temp.68.2F

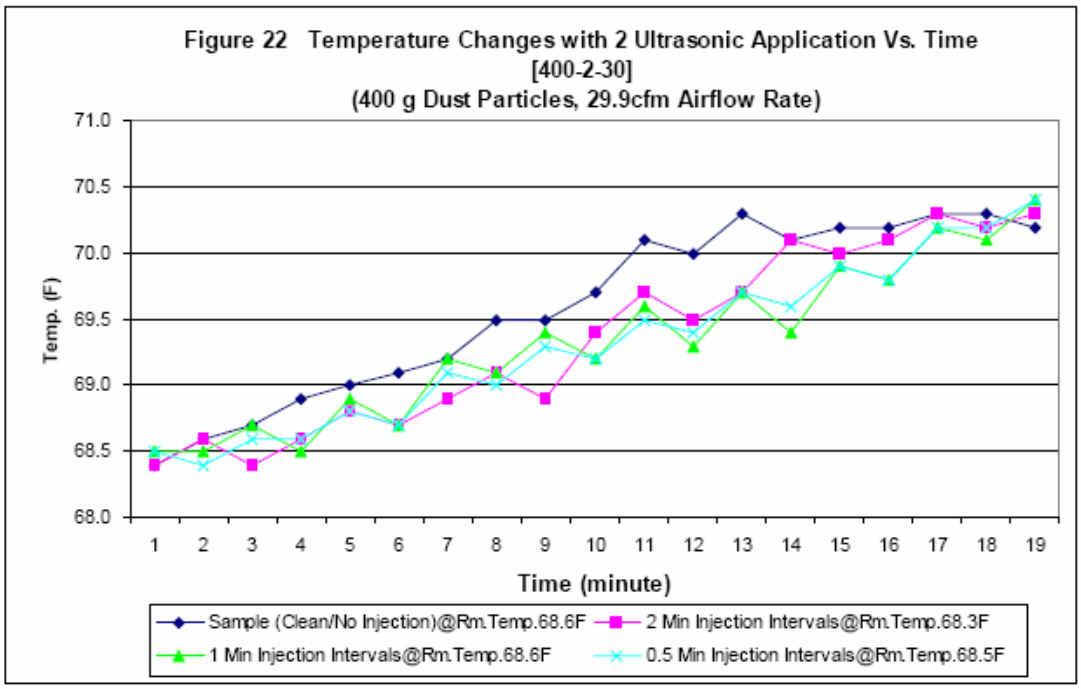
Figure 22 Temperature Changes with 2 Ultrasonic Application Vs. Time
[400-2-30]
(400 g Dust Particles, 29.9cfm Airflow Rate)
Temp. (F)
71.0
70.5
70.0
69.5
69.0
68.5
68.0
1 2 3 4 5 6 7 8 9 10 11 12 13 14 15 16 17 18 19
Time (minute)
Sample (Clean/No Injection)@Rm.Temp.68.6F
2 Min Injection Intervals@Rm.Temp.68.3F
1 Min Injection Intervals@Rm.Temp.68.6F
0.5 Min Injection Intervals@Rm.Temp.68.5F

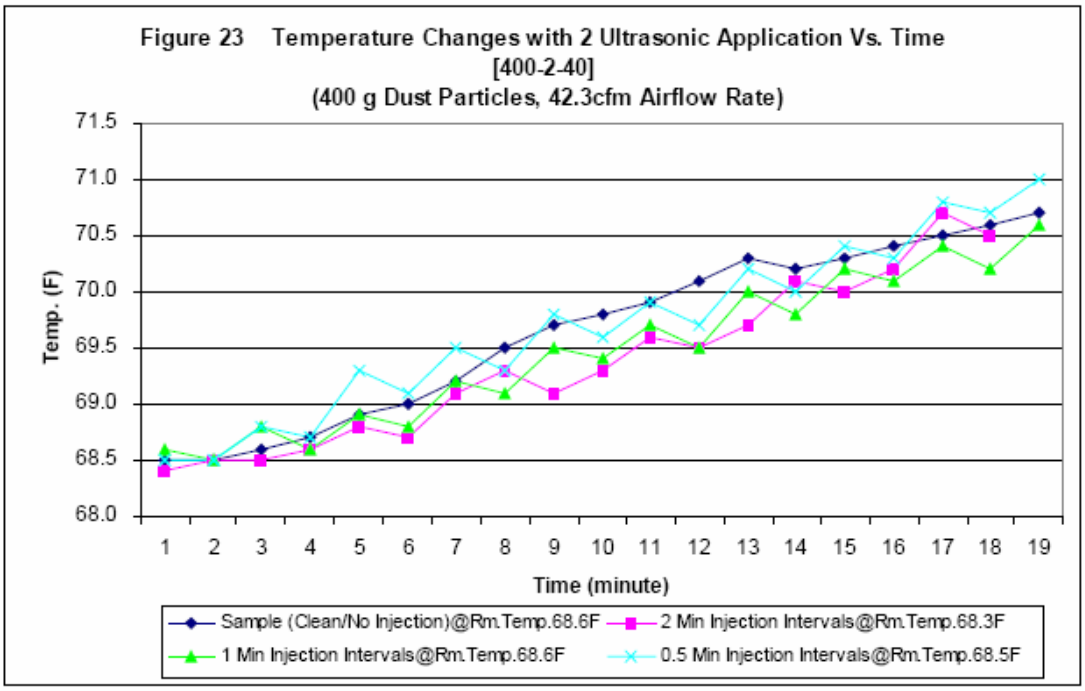
Figure 23 Temperature Changes with 2 Ultrasonic Application Vs. Time
[400-2-40]
(400 g Dust Particles, 42.3cfm Airflow Rate)
Temp. (F)
71.5
71.0
70.5
70.0
69.5
69.0
68.5
68.0
1 2 3 4 5 6 7 8 9 10 11 12 13 14 15 16 17 18 19
Time (minute)
Sample (Clean/No Injection)@Rm.Temp.68.6F
2 Min Injection Intervals@Rm.Temp.68.3F
1 Min Injection Intervals@Rm.Temp.68.6F
0.5 Min Injection Intervals@Rm.Temp.68.5F

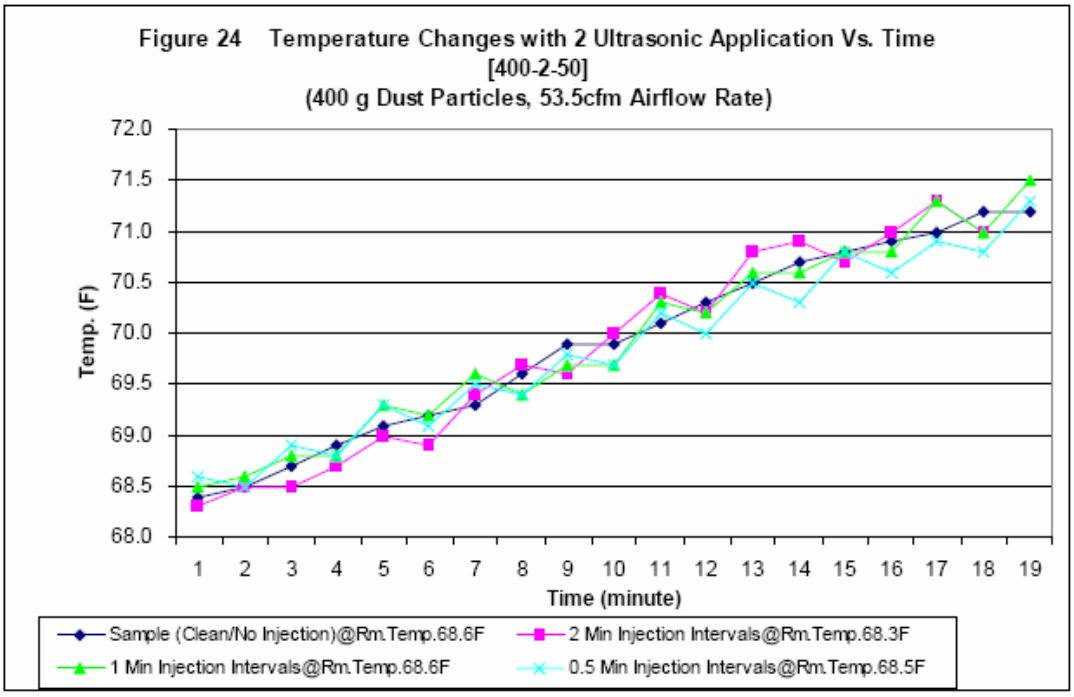
Figure 24 Temperature Changes with 2 Ultrasonic Application Vs. Time
[400-2-50]
(400 g Dust Particles, 53.5cfm Airflow Rate)
Temp. (F)
72.0
71.5
71.0
70.5
70.0
69.5
69.0
68.5
68.0
1 2 3 4 5 6 7 8 9 10 11 12 13 14 15 16 17 18 19
Time (minute)
Sample (Clean/No Injection)@Rm.Temp.68.6F
2 Min Injection Intervals@Rm.Temp.68.3F
1 Min Injection Intervals@Rm.Temp.68.6F
0.5 Min Injection Intervals@Rm.Temp.68.5F

Appendix II

Table A-1. Experiment Results of Comparison Tests on Coated/Uncoated Thermal Couple

Time	Air flow: 15 voltage control ammonia/water: 2ml/min Particles: 75 gram		Air flow: 10 voltage control ammonia/water: 2ml/min Particles: 75 gram		Air flow: 15 voltage control ammonia/water: 3ml/min Particles: 75 gram	
	coated	original	coated	original	coated	original
0	26.2	20.0	201.1	312.8	118.3	54.6
1	237.8	311.7	368.3	462.8	147.8	71.0
2	384.6	380.0	455.8	520.0	171.7	84.3
3	474.4	495.3	504.0	545.6	201.7	100.9
4	538.9	533.1	537.8	573.9	225.6	114.2
5	571.1	579.4	556.1	588.9	288.9	149.4
10	650.6	654.4	627.8	651.1	332.6	358.5
15	694.4	702.8	672.8	690.6	552.2	559.4
20	728.3	734.4	707.2	720.0	630.0	640.0
25	754.4	762.8	732.2	745.6	678.9	687.8
30	776.1	782.8	761.1	766.7	710.6	720.6
35	795.6	803.9	773.3	778.3	735.0	744.4
40	813.3	821.7	793.9	797.2	767.8	777.8
45	827.8	836.1	809.4	809.4	780.6	790.0
50	842.8	850.6	825.0	818.3	790.6	800.6
55	853.3	861.1	833.9	832.2	800.6	809.4
60	863.3	871.1	840.6	843.3	808.9	819.4
65	871.7	879.4	848.9	850.6	815.6	825.0
70	876.7	884.4	856.1	857.2	821.1	830.0
75	878.3	886.7	861.1	862.2	822.2	832.2
80	881.1	890.0	866.7	870.6	827.2	835.6
85	868.3	878.9	875.6	876.7		
90	863.9	875.0	882.2	883.3		

95	868.9	878.9	886.7	887.8		
100	866.7	879.4	890.0	890.6		
105	869.4	877.8	894.4	895.0		
110			898.9	898.3		
115			902.2	901.7		
120			906.1	903.9		
125			908.3	906.7		

Table A-2: Experiment Results of Comparison Tests on Coated/Uncoated Thermal Couple with DAS

Time	Test # 4		Test # 5		Test # 6		Test # 7		Test # 8	
	A02	A04	A02	A04	A02	A04	A02	A04	A02	A04
minute	°C	°C	°C	°C	°C	°C	°C	°C	°C	°C
1	232.0	202.7	22.9	23.0	22.8	22.8	22.3	22.3	22.1	21.9
2	297.8	293.5	23.0	23.0	22.9	22.9	35.4	35.2	112.4	98.1
3	459.3	486.0	22.9	23.0	22.8	22.7	141.9	149.9	207.8	205.8
4	555.9	592.9	22.9	22.9	22.8	22.8	233.6	259.1	270.8	283.0
5	610.1	647.9	22.9	22.9	22.8	22.8	296.3	329.2	310.3	331.7
6	643.2	680.1	46.2	51.3	22.8	22.8	337.4	369.7	333.5	360.0
7	665.8	701.8	189.7	201.1	22.8	22.8	363.0	392.2	351.8	379.8
8	683.5	716.5	306.9	309.2	22.8	22.9	378.9	405.3	365.1	393.8
9	698.0	730.1	383.7	374.1	22.8	22.9	389.0	412.6	374.4	403.3
10	711.1	741.9	427.6	413.9	22.8	22.8	397.2	418.9	378.7	409.2
11	722.1	751.8	453.7	454.0	22.8	22.8	402.3	423.0	382.6	412.9
12	732.3	760.9	471.2	476.0	72.6	72.4	407.3	426.4	387.7	418.3
13	741.3	769.3	483.2	483.0	193.8	213.8	409.2	428.4	391.7	422.4
14	749.3	776.6	493.7	494.0	287.9	326.7	412.9	430.3	395.3	426.2
15	756.5	783.1	501.2	509.0	352.3	395.3	415.6	432.4	397.8	429.1
16	763.1	789.1	506.1	509.0	389.0	425.1	417.9	434.4	399.2	431.2
17	768.8	794.3	512.4	511.0	411.2	436.5	420.6	436.4	401.0	432.9
18	774.2	799.4	516.4	527.0	426.1	446.9	422.8	438.6	402.2	434.5
19	779.1	804.0	521.8	536.0	438.6	456.4	424.2	439.7	404.8	436.8
20	784.0	808.5	526.6	542.0	444.7	460.7	425.7	440.4	405.9	438.3
21	788.5	812.6	532.3	551.0	448.4	464.0	426.8	440.8	407.5	439.9
22	792.9	816.7	536.4	558.5	451.7	466.5	427.8	443.0	409.2	441.0

23	797.0	820.4	543.8	566.7	454.6	469.4	428.8	443.4	411.4	443.0
24	801.0	824.0	546.9	569.5	458.2	472.5	430.1	443.5	410.0	443.2
25	802.9	826.3	550.5	572.4	461.2	476.1	430.2	444.0	412.1	444.5
26	806.0	829.1	554.3	575.3	470.2	481.8	429.7	443.5	414.0	446.1
27	809.4	832.3	557.6	577.8	477.1	488.7	430.9	444.4	413.3	446.3
28	812.3	834.9	559.8	578.9	482.7	493.5	430.6	443.9	415.0	448.0
29	815.3	837.7	563.6	581.1	486.1	496.5	432.3	445.8	416.1	448.3
30	818.0	840.3	568.5	582.6	488.5	499.1	432.3	445.6	438.7	465.9
31	820.7	842.7	570.8	584.7	488.6	501.6	433.4	447.6	466.2	492.9
32	823.4	845.3	573.0	586.5	490.2	503.6	433.5	446.4	485.0	511.2
33	826.0	847.7	575.4	589.2	492.7	505.6	433.5	446.0	496.1	523.2
34	828.1	849.6	577.6	591.2	494.1	506.6	433.4	447.0	504.4	532.4
35	829.7	851.2	579.2	593.5	495.7	508.1	434.1	447.0	511.0	538.8
36	831.7	853.2	582.2	596.4	497.2	509.2	435.0	447.1	514.6	543.2
37	833.4	854.7	584.3	598.3	498.4	510.2	434.8	447.6	516.5	546.1
38	835.3	856.5	586.4	599.3	499.4	511.6	435.3	447.4	521.9	550.0
39	837.4	858.4	587.3	600.0	500.7	511.9	435.2	447.8	524.8	553.4
40	839.0	859.9	588.3	601.7	502.0	513.6	435.2	448.0	528.6	557.0
41	841.1	861.7	590.2	603.3	503.3	514.6	435.7	448.2	532.3	560.7
42	842.5	863.1	591.7	604.7	504.5	515.7	435.9	448.4	534.8	563.0
43	844.6	865.0	593.0	605.3	506.9	517.2	436.2	448.9	536.6	565.1
44	845.9	866.3	594.7	607.2	507.7	517.7	435.9	448.1	537.6	566.5
45	847.3	867.6	595.4	607.9	508.4	518.3	435.3	447.1	539.1	568.1
46	850.3	870.1	596.7	609.0	509.4	518.5	436.0	447.8	539.9	569.7
47	859.8	877.5	598.3	609.9	510.0	519.2	436.0	448.2	542.2	571.1
48	863.3	881.1	598.0	609.9	511.7	521.1	436.0	448.1	542.8	572.1
49	858.1	877.5	598.4	610.3	513.4	523.0	436.6	448.5	544.0	573.4

50	853.3	873.4	600.3	611.5	530.7	541.9	436.2	447.7	544.1	574.4
51	849.9	890.2	600.3	611.9	544.7	556.6	435.9	448.2	559.4	581.3
52			601.3	613.1	553.5	565.3	436.0	448.5	585.4	602.7
53			602.3	613.5	560.2	572.1	436.2	448.5	599.6	616.8
54			604.5	615.4	566.0	577.6	436.6	448.5	608.1	625.6
55			606.0	617.0	569.9	582.0	435.7	448.2	614.8	632.5
56			607.8	618.5	573.4	584.8	435.8	448.4	621.1	638.4
57			608.6	619.4	576.4	587.2	436.9	448.0	623.4	642.6
58			609.5	620.5	578.5	589.3	436.7	448.0	628.5	647.1
59			610.7	621.5	581.3	592.5	435.6	447.2	631.5	650.8
60			610.9	621.3	583.8	594.6	435.0	447.9	635.1	654.2
61			611.7	622.1	586.5	596.6	435.3	448.0	636.2	656.3
62			611.7	622.2	589.0	600.2	436.4	449.0	638.5	658.3
63			612.5	622.5	591.7	602.3	437.3	449.2	640.5	659.1
64			612.3	622.1	594.3	605.5	437.2	449.2	640.7	660.1
65			613.1	622.8	596.8	607.5	436.3	448.1	643.0	662.4
66			613.5	623.4	599.7	610.6	436.0	448.9	644.9	664.1
67			614.1	624.1	602.6	613.3	437.2	449.6	646.6	665.6
68			618.1	631.7	604.4	615.3	438.4	450.7	647.5	666.6
69			623.5	636.5	605.8	616.9	439.0	451.0	649.5	668.3
70			627.0	639.7	607.6	618.1	439.5	452.0	650.4	669.7
71			629.6	642.4	609.0	619.6	439.3	451.5	651.7	671.2
72			631.1	643.3	610.5	620.3	439.8	452.0	652.9	672.1
73			633.2	645.7	610.8	620.8	439.4	451.0	655.1	673.9
74			635.1	647.3	611.9	622.0	440.0	451.4	656.8	675.8
75			637.1	648.8	612.6	622.1	441.4	452.6	656.5	676.3
76			637.9	649.6	613.2	622.1	442.0	452.9	657.0	677.1

77			639.6	651.0	614.1	623.1	443.4	454.0	657.5	677.5
78			640.1	651.4	614.9	623.6	444.2	454.2	657.9	678.1
79			640.2	651.2	614.7	623.6	445.1	454.8	658.9	678.9
80			640.5	651.4	615.0	623.7	445.8	455.8	659.5	679.7
81			641.1	652.0	615.7	624.4	445.2	455.6	661.1	680.9
82			640.8	651.6	617.0	626.1	445.2	455.6	663.7	683.0
83			641.6	652.2	618.4	627.6	446.1	456.1	664.8	684.3
84			641.4	652.5	619.9	628.7	447.0	456.5	665.4	685.0
85			642.6	653.1	620.4	629.3	447.3	457.4	665.0	685.5
86			643.0	653.8	621.8	631.1	447.8	458.1	665.8	686.4
87			643.4	654.4	623.6	632.5	448.0	457.9	665.4	685.8
88			645.2	655.8	624.6	633.2	447.6	456.8	665.6	686.1
89			645.9	657.2	625.2	633.9	447.1	456.2	666.9	686.8
90			646.7	658.3	626.5	635.0	446.9	457.2	666.7	687.1
91			648.4	659.7	627.1	635.8	447.0	456.6	665.7	686.9
92			649.6	660.1	627.3	636.1	446.0	455.8	667.3	687.7
93			649.7	660.5	627.9	636.4	446.8	456.6	666.1	687.6
94			650.9	661.8	628.5	636.7	446.3	456.1	666.5	688.1
95			651.8	662.2	628.6	636.7	447.7	457.8	667.6	688.6
96			652.1	662.7	628.4	636.8	447.3	457.1	667.4	688.8
97			652.5	663.5	628.3	635.9	448.4	458.3	669.8	690.5
98			653.6	664.2	628.5	636.3	448.2	457.8	672.4	692.6
99			654.2	665.2	628.9	636.2	449.1	458.5	671.5	692.8
100			655.2	665.8	629.0	635.8	448.9	458.9	670.4	691.9
101			655.2	665.6	628.6	635.8	450.5	459.9	672.9	693.5
102			655.7	666.3	628.9	636.2	449.8	459.3	674.2	695.1
103			655.5	665.8	628.9	635.9	449.3	459.5	675.3	697.3

104			656.4	666.7	628.6	635.2	449.3	458.4	676.1	698.3
105			657.4	667.4	628.3	634.6	448.4	457.8	677.4	699.4
106			657.5	667.9	629.0	635.4	448.9	458.5	678.2	699.8
107			657.2	667.4	628.7	635.3	448.6	458.3	684.0	703.6
108			657.0	667.5	629.2	635.2	449.4	458.8	692.1	710.7
109			657.3	667.2	629.2	636.0	449.5	458.3	697.5	716.1
110			656.8	666.9	629.9	636.4	449.6	459.2	702.1	721.0
111			657.0	666.6	629.8	636.2	449.7	459.7	706.8	724.8
112			656.7	666.8	630.3	636.3	449.6	459.2	708.7	726.8
113			656.2	666.3	630.3	636.8	449.0	458.1	711.7	729.5
114			656.9	667.2	631.4	637.6	449.2	458.3	715.4	732.8
115			657.6	668.0	631.3	637.4	449.7	459.1	715.6	734.3
116			658.1	668.5	632.1	638.1	449.1	458.4	716.1	734.5
117			658.9	668.9	631.7	637.7	448.2	457.7	715.8	734.8
118			658.7	668.4	632.2	638.0	448.1	457.5	716.1	734.9
119			658.0	668.0	632.7	638.1	449.6	459.3	717.2	735.7
120			657.7	667.5	632.6	638.2	449.8	458.8	718.1	736.6
121			657.6	667.8	632.9	638.5	450.8	459.8	719.5	737.8
122			658.4	668.1	633.0	638.8	449.4	458.8	720.5	738.8
123			659.2	668.6	633.2	638.7	449.0	458.8	721.9	740.2
124			659.1	669.1	632.9	639.1	449.6	459.2	724.1	742.0
125			659.4	669.1	633.7	639.1	449.1	457.9	724.9	743.2
126			660.0	670.2	634.0	639.7	448.1	457.7	726.3	744.6
127			661.0	670.8	634.5	639.3	448.2	458.1	728.4	746.1
128			662.3	672.6	634.1	639.9	448.2	457.6	730.2	747.6
129			663.4	673.2	634.6	640.1	448.5	458.1	731.2	748.7
130			663.2	672.9	634.8	640.7	448.5	458.2	732.8	750.4

131			662.6	672.3	635.6	641.4	449.5	459.0	735.6	752.6
132			661.8	671.1	636.2	642.5	454.5	463.7	737.4	754.6
133			660.9	670.4	637.7	644.5	480.7	491.9	739.7	756.2
134			661.3	671.0	639.5	646.2	500.7	511.6	741.1	757.5
135			662.0	671.6	640.9	647.6	513.0	523.9	741.8	758.4
136			662.3	672.0	641.2	647.5	521.4	532.0	742.6	759.3
137			662.8	672.7	640.9	647.1	528.7	539.2	740.8	758.2
138			663.8	673.6	640.5	646.7	532.6	543.0	738.9	756.9
139			663.9	673.7	639.4	644.5	557.8	571.1	737.8	756.2
140			662.0	672.1	638.9	643.7	596.9	612.0	738.2	756.2
141			661.1	670.9	638.3	643.1	620.6	637.3	738.8	756.4
142			661.1	671.0	638.4	643.4	637.6	654.6	738.4	756.3
143			660.0	669.8	638.8	644.2	649.8	667.4		
144			660.1	669.5	639.0	644.3	659.9	677.6		
145			660.0	670.5	638.7	644.5	668.1	686.0		
146			661.2	670.8	639.0	644.5	675.7	693.0		
147			661.2	671.0	639.5	644.8	681.7	699.0		
148			661.5	671.6	639.8	645.1	687.1	704.3		
149			661.9	671.7	640.4	645.4	692.7	709.6		
150			661.7	671.2	640.3	645.7	697.8	714.7		
151			661.7	671.4	639.9	645.6	702.7	719.2		
152			661.6	671.0	640.3	645.7	707.1	723.6		
153			660.1	670.0	640.4	645.8	710.6	727.1		
154			659.8	669.7			714.5	730.6		
155			660.2	669.8			718.1	734.2		
156			659.6	669.5			721.7	737.6		
157			660.9	671.1			725.4	741.1		

158			660.8	670.2			727.7	743.4		
159			660.8	671.0			730.4	746.2		
160			661.7	671.4			733.7	749.0		
161			662.0	671.8			736.9	752.1		
162			661.0	670.6			739.5	754.4		
163			660.9	670.0			742.1	756.9		
164			660.2	669.5			745.0	759.8		
165			659.9	669.4			747.3	762.1		
166			660.0	669.5			748.7	763.5		
167			660.1	669.5			749.9	764.3		
168			660.1	670.0			749.9	764.2		
169			660.8	670.5			751.7	765.9		
170			661.1	670.8			754.9	768.9		
171			661.5	670.9			757.1	771.0		
172			660.3	669.9			758.8	772.6		
173			659.8	669.2			760.7	774.4		
174			659.8	669.3			761.5	775.6		
175			659.6	669.1			763.3	777.1		
176			662.8	673.3			764.8	778.3		
177			663.7	675.4			766.1	779.6		
178			665.5	677.2			767.3	780.8		
179			667.0	678.6			767.7	781.0		
180			665.0	682.0			768.2	781.3		
181			667.3	685.4			767.7	781.2		
182			669.6	686.9			768.0	781.4		
183							768.8	782.0		
184							768.7	781.9		